Research Paper

THEMED ISSUE: Tectonic, Sedimentary, Volcanic and Fluid Flow Processes along the Queen Charlotte-Fairweather Fault System and Surrounding Continental Margin

GEOSPHERE

GEOSPHERE

https://doi.org/10.1130/GES02359.1

14 figures; 1 set of supplemental files

CORRESPONDENCE: james.baichtal@usda.gov

CITATION: Baichtal, J.F., Lesnek, A.J., Carlson, R.J., Schmuck, N.S., Smith, J.L., Landwehr, D.J., and Briner, J.P., 2021, Late Pleistocene and early Holocene sea-level history and glacial retreat interpreted from shell-bearing marine deposits of southeastern Alaska, USA: Geosphere, https://doi.org/10.1130/GES02359.1.

Science Editor: Shanaka de Silva
Guest Associate Editor: Daniel Brothers

Received 30 September 2020
Revision received 9 March 2021
Accepted 9 July 2021

Published online 8 November 2021

Late Pleistocene and early Holocene sea-level history and glacial retreat interpreted from shell-bearing marine deposits of southeastern Alaska, USA

James F. Baichtal[1], Alia J. Lesnek[2], Risa J. Carlson[3], Nicholas S. Schmuck[4], Jane L. Smith[5], Dennis J. Landwehr[1], and Jason P. Briner[6]

[1]Tongass National Forest, Ketchikan, Alaska 99901, USA
[2]Department of Earth Sciences, University of New Hampshire, Durham, New Hampshire 03824, USA
[3]Tongass National Forest, Thorne Bay, Alaska 99901, USA
[4]Department of Anthropology, University of Alaska Fairbanks, Fairbanks, Alaska 99775, USA
[5]Tongass National Forest, Petersburg, Alaska 99833, USA
[6]Department of Geology, University at Buffalo, Buffalo, New York 14209, USA

ABSTRACT

We leverage a data set of >720 shell-bearing marine deposits throughout southeastern Alaska (USA) to develop updated relative sea-level curves that span the past ~14,000 yr. This data set includes site location, elevation, description when available, and 436 ^{14}C ages, 45 of which are published here for the first time. Our sea-level curves suggest a peripheral forebulge developed west of the retreating Cordilleran Ice Sheet (CIS) margin between ca. 17,000 and 10,800 calibrated yr B.P. By 14,870 ± 630 to 12,820 ± 340 cal. yr B.P., CIS margins had retreated from all of southeastern Alaska's fjords, channels, and passages. At this time, isolated or stranded ice caps existed on the islands, with alpine or tidewater glaciers in many valleys. Paleoshorelines up to 25 m above sea level mark the maximum elevation of transgression in the southern portion of the study region, which was achieved by 11,000 ± 390 to 10,500 ± 420 cal. yr B.P. The presence of Pacific sardine (*Sardinops sagax*) and the abundance of charcoal in sediments that date between 11,000 ± 390 and 7630 ± 90 cal. yr B.P. suggest that both ocean and air temperatures in southeastern Alaska were relatively warm in the early Holocene. The sea-level and paleoenvironmental reconstruction presented here can inform future investigations into the glacial, volcanic, and archaeological history of southeastern Alaska.

Jim Baichtal https://orcid.org/0000-0003-3876-3110

INTRODUCTION

The northern Pacific margin of the United States and Canada has undergone rapid and spatially variable changes in sea level since the Last Glacial Maximum (Clark et al., 2009) owing to the complex interactions between climate and the solid earth (Shugar et al., 2014). These interactions are numerous, including isostatic adjustment caused by the advance and retreat of the Cordilleran Ice Sheet (CIS; e.g., Lesnek et al., 2020), eustatic sea-level change related to the decay of global glacier complexes (Lambeck et al., 2014), and tectonism along the Pacific–North American plate boundary (e.g., Barrie et al., 2021). Regionally resolved reconstructions of sea-level fluctuations can provide insight into the relative roles of these processes on landscape change.

Sea-level reconstructions also serve as a key component of investigations into early human occupation of the northwestern North American Pacific coast, including the initial migration into the Americas during the Late Pleistocene (Braje et al., 2020). Detailed sea-level histories and high-resolution topographic and bathymetric data have successfully guided archaeological surveys near the modern Pacific coastline (Baichtal and Carlson, 2010; Carlson, 2012; Carlson and Baichtal, 2015; McLaren et al., 2014, 2018, 2020), leading to the discovery of dozens of cultural sites across southeastern Alaska (USA) (Carlson, 2012; Carlson and Baichtal, 2015) and British Columbia (Canada) (Letham et al., 2016; Fedje et al., 2018; Mackie et al., 2018). Indeed, these techniques have uncovered the oldest evidence to date of human presence on the Pacific coast of North America: a set of footprints on Calvert Island, British Columbia, that date to ca. 13,200 calibrated yr B.P. (McLaren et al., 2014, 2018). These findings demonstrate that highly resolved sea-level reconstructions are a powerful tool in the search for ancient cultural sites along the northwestern North American Pacific coast.

Here, we present an updated postglacial relative sea-level history for coastal southeastern Alaska (Fig. 1). We begin by documenting the reported and known occurrences of shell-bearing raised marine sediments (hereafter referred to as shell-bearing strata) across southeastern Alaska, from Yakutat to the northern shores of Haida Gwaii, British Columbia (Fig. 2). We then present 45 new ^{14}C ages on shells from these deposits. Combining this data set with previously published sea-level constraints, we develop new sea-level curves for 11 areas in southeastern Alaska, which give insight into the region's complex isostatic and eustatic sea-level history. We also report the presence of environmental (i.e., non-anthropogenic) charcoal and Pacific sardine (*Sardinops sagax*) in select deposits, which

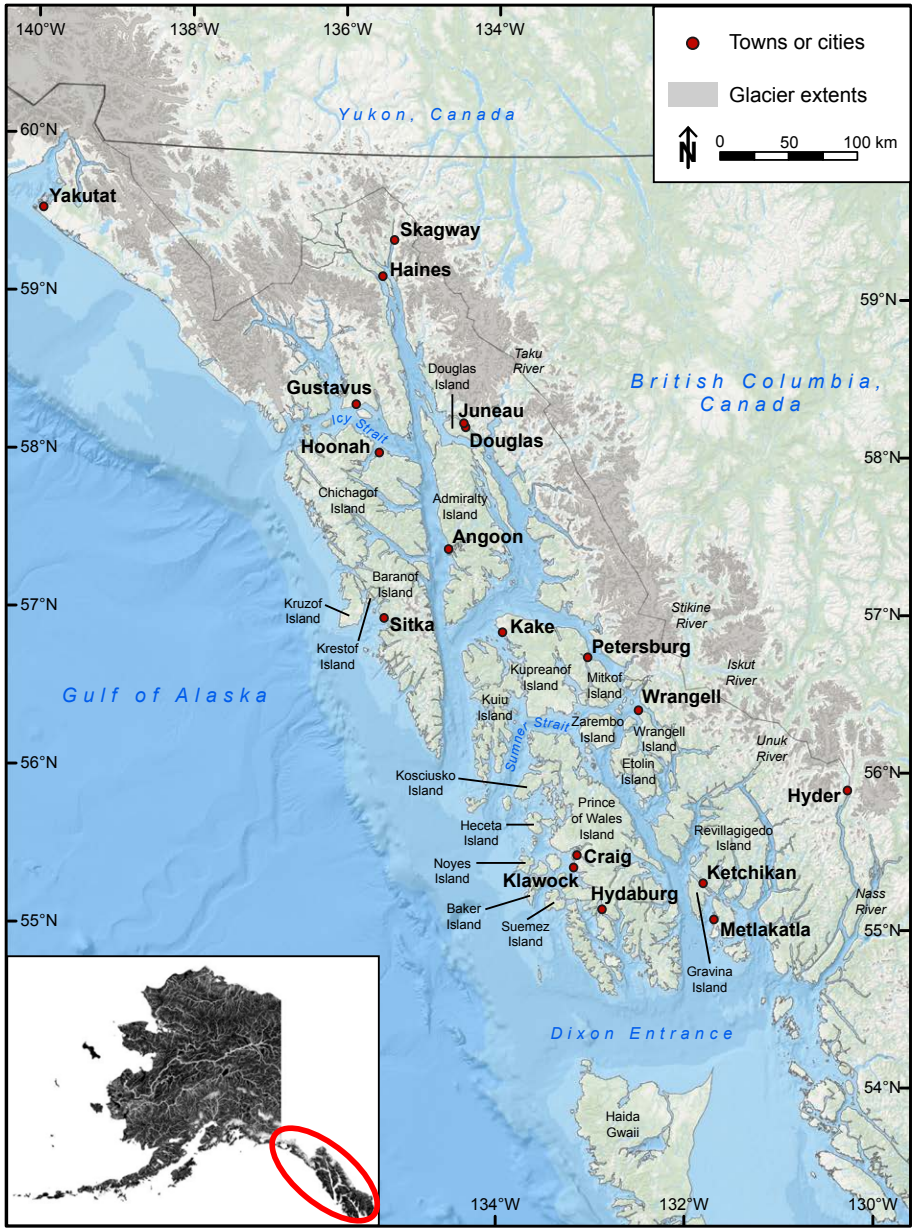

Figure 1. Coastal outline of northwestern British Columbia, Canada, and southeastern Alaska, USA. The study area encompasses the map extent. Shown are the locations of the islands, towns, and the extent of the existing glaciers (gray shading) within the study area.

we use to infer the timing of the regional Holocene Climatic Optimum. Finally, we discuss the potential impact of these sea-level changes on early human occupation of coastal southeastern Alaska.

BACKGROUND

Regional Setting

Our study area includes the lands within the boundaries of the Tongass National Forest and Glacier Bay National Park, specifically from Yakutat Bay to Dixon Entrance and the northern shores of Haida Gwaii, and from the Queen Charlotte fault into the transboundary river valleys of British Columbia (Fig. 2). The study area roughly includes all of the Alexander Archipelago, extending 850 km from the northwest to the southeast and 270 km west to east (Fig. 1). The Alexander Archipelago includes ~1100 islands and 16,000 km of coastline. The landscape of the archipelago rises abruptly from the sea, commonly reaching elevations of 1000 m above sea level (asl) within 2 km of tidewater. The region receives nearly continuous storms, owing to a semi-permanent low-pressure system in the Gulf of Alaska. Precipitation amounts vary from 150 to 750 cm of precipitation annually. Bedrock geology in southeastern Alaska consists mainly of volcanic and sedimentary deposits representing a succession of magmatic arcs ranging in age from the Neoproterozoic to the present, intruded by plutons related to the formation, deformation, and rifting of the successive arcs (Wilson et al., 2015). The Neoproterozoic, Paleozoic, and Mesozoic arcs were long-lived oceanic arcs (S.M. Karl, 2020, personal commun.), which today exist on a complex assemblage of accreted terranes. The morphology of the mountains in the region, as well as that of the many straits, passages, and channels that separate the islands, broadly reflects the underlying geologic structure but has been greatly modified by Pleistocene glaciation.

During the Late Pleistocene, much of southeastern Alaska was covered by the CIS (Dyke, 2004). Recent investigations have provided chronological constraints on both the extent and retreat of

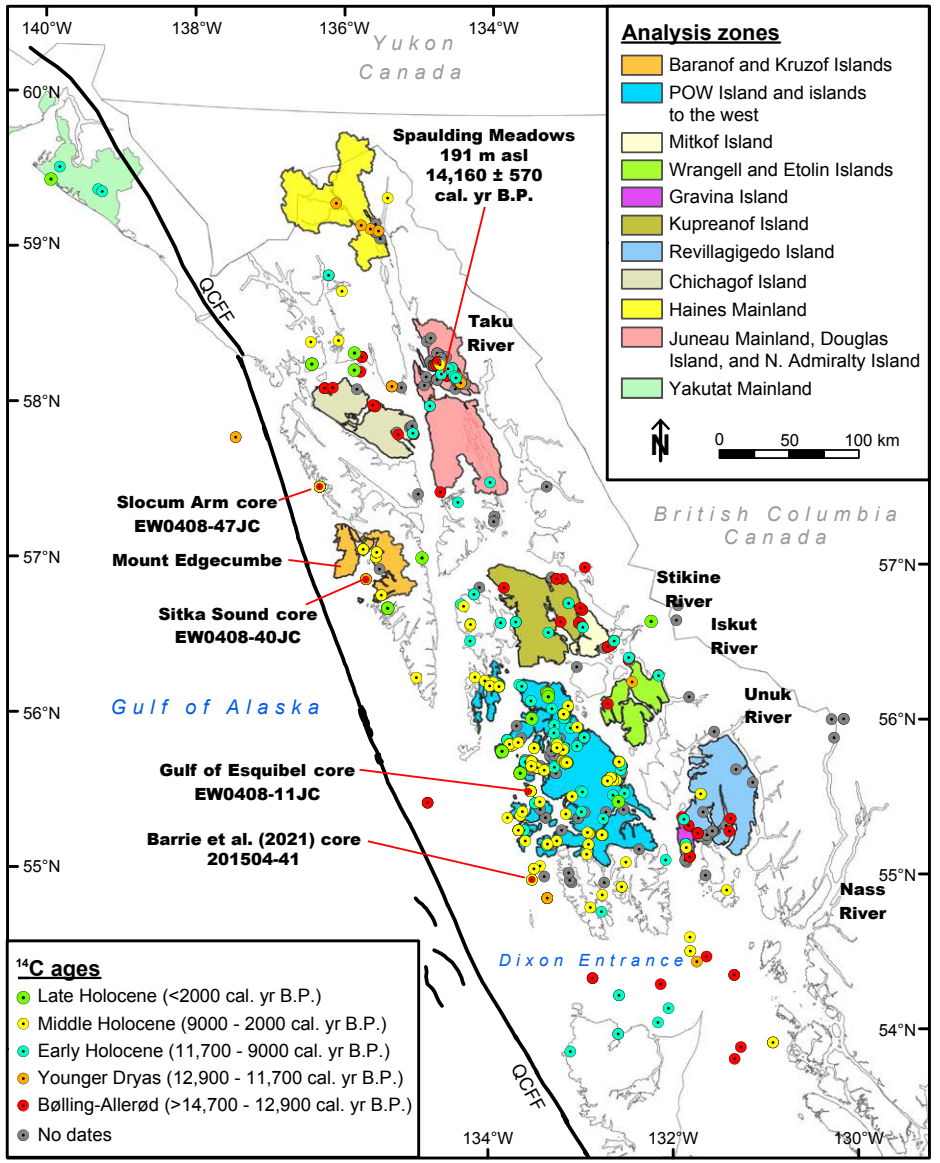

Figure 2. Coastal outline of northwestern British Columbia, Canada, and southeastern Alaska, USA, showing the locations of the shell-bearing strata sample sites across the study area. The sites are color coded by age: Bølling-Allerød (ca. 14,700–12,900 calibrated yr B.P.), Younger Dryas (12,900–11,700 cal. yr B.P.), early Holocene (11,700–9000 cal. yr B.P.), middle Holocene (9000–2000 cal. yr B.P.), and late Holocene (2000 to ca. 200 cal. yr B.P.). The 11 analysis zones discussed in the text and shown in Figures 3A to 3K are color coded. QCFF—Queen Charlotte–Fairweather fault system; asl—above sea level; POW—Prince of Wales Island.

the CIS in this region. Cosmogenic ^{10}Be ages from the westernmost islands of southeastern Alaska and ^{14}C-dated animal bones from an ice-overrun cave on northern Prince of Wales Island suggest the maximum extent of the CIS occurred between ca. 20,000 and ca. 17,000 cal. yr B.P. (Lesnek et al., 2018; ^{14}C ages were recalibrated using the Marine20 calibration curve and an updated marine reservoir correction; see below). Additional ^{10}Be ages from other islands around southeastern Alaska indicate that the fjords and straits were deglaciated by ca. 14,900 cal. yr B.P., after which the CIS margins transitioned to being primarily land-terminating (Lesnek et al., 2020). Small, independent, remnant ice caps may have persisted in high-elevation areas until the early Holocene (Lesnek et al., 2020), although the history of these glaciers remains poorly constrained.

Today, within the bounds of the study area, spanning the United States and Canadian Coast Range, the Tongass National Forest, and Glacier Bay National Park, glaciers cover >28,000 km^2 (RGI Consortium, 2017). Baranof Island, in the western portion of the archipelago, hosts small glaciers that are likely remnants of Little Ice Age (1250–1850 CE) glacial advance (Gaglioti et al., 2019). Many areas throughout southeastern Alaska are still rebounding as the result of post–Little Ice Age melting, with uplift rates varying from 10 to 32 mm yr^{-1} (Larsen et al., 2004, 2005). Continued thinning of the existing tidewater glaciers is resulting in accelerated uplift, particularly in the vicinity of Juneau (Larsen et al., 2004, 2005, 2007; Trüssel et al., 2013).

Previous Work

Shell-bearing fossiliferous marine deposits have long been observed and recorded throughout southeastern Alaska (Buddington and Chapin, 1929). These deposits have been referred to as uplifted marine sediments and terraces, fossiliferous marine gravel, sand, and clay, and glaciomarine sediments. The first detailed description of such deposits on Douglas Island came from W.H. Dall on the 1899 Harriman Alaska Expedition. Dall (1904) recognized the similarity between these sediments in southeastern Alaska and Pleistocene marine deposits in eastern

North America. Subsequent research focused on cataloging the occurrences of raised marine deposits around Juneau (e.g., Knopf, 1912; Twenhofel, 1952). Miller (1972, 1973a, 1973b, 1975) characterized these facies and named these shell-bearing strata the Gastineau Channel Formation. Others further documented elevated shell-bearing marine clays in their evaluations of earthquake and other geologic hazards to coastal communities of southeastern Alaska (Lemke and Yehle 1972a, 1972b; Lemke, 1974a, 1974b, 1975; Yehle and Lemke, 1972; Yehle, 1974, 1978, 1979). Sainsbury (1961) and Swanston (1969) described marine till with shell fragments and a raised marine beach on Prince of Wales Island. Similarly, Loney (1964) described fossil-bearing marine glacial clay in stream valleys at various elevations on Admiralty Island. On Gravina Island, Berg (1973) described uplifted glacial-marine deposits. These authors recognized these deposits as evidence of a postglacial marine transgression on isostatically depressed lands.

Mobley (1988) developed Holocene sea-level curves for Heceta and Prince of Wales Islands based on a limited data set and compared these deposits to those described by Clague et al. (1982a). Mobley concluded that the Heceta Island sea-level curve was comparable to that of Haida Gwaii. Mann and Hamilton (1995) recognized the marine transgression described by Mobley (1988) and a transgression of similar magnitude and duration to that of Haida Gwaii archipelago (formerly the Queen Charlotte Islands). Putnam and Fifield (1995) documented raised shell-bearing strata for many of the estuaries on Prince of Wales Island, plotting coastal emergence gradients. Mann and Streveler (2008) and Connor et al. (2009) characterized the occurrence of shell-bearing strata and the glacial and relative sea-level history of the Icy Strait region. The highest reported occurrence of glaciomarine sediments in southeastern Alaska is from Montana Creek near Juneau at 228.6 m asl. The highest documented occurrence of shell-bearing strata containing foraminifera is exposed in a landslide scarp on Admiralty Island noted by Miller (1973a) at an elevation of 211.8 m asl; no date has been obtained from this site. The highest occurrences of sampled and dated shell-bearing strata are at 191.0 m asl at Spaulding Meadows near Juneau. These two samples date to 13,950 ± 520 cal. yr B.P. and 14,160 ± 570 cal. yr B.P. U.S. Forest Service archaeologists have documented raised shell-bearing strata in southeastern Alaska since the mid-1980s (Carlson, 1984, 1991, 1992; Campbell, 1995; Davis, 1990; Davis et al., 1991; Putnam and Fifield, 1995). Hastings (2005) developed geologic and biologic models along three elevation breaks based on geologic evidence and the occurrences of coastal cutthroat trout (*Oncorhynchus clarki clarki*) and Dolly Varden (*Salvelinus malma*) believed to have been isolated by postglacial isostatic rebound.

In 2004, the Tongass National Forest geology program began a focused effort to document and date raised shell-bearing strata across the region. Subsets of these data were published in Hastings (2005), Carlson (2007, 2012), Shugar et al. (2014), and Schmuck et al. (2021). This manuscript is the first instance where the complete data set is compiled; the data set includes 723 samples, 436 ^{14}C ages (45 of which are new), and 110 new sites. The sea-level curves presented here further define the complexity of postglacial relative sea-level fluctuations published by Shugar et al. (2014) through the addition of 110 new data points, more precise elevation controls, and updated, locally derived marine reservoir correction values (see below). We use this updated data set to refine the region's glacial and isostatic history (Lesnek et al., 2020). Similar glacially induced crustal displacement and relative sea-level changes have been well documented along the coastal margins of British Columbia (Clague et al., 1982; Clague, 1983; Luternauer et al.,1989; Josenhans et al., 1995, 1997; Fedje and Christensen, 1999; Fedje and Josenhans, 2000; Barrie and Conway, 2002; James et al., 2002; Hetherington et al., 2003, 2004; Hetherington and Barrie, 2004; McLaren, 2008; McLaren et al., 2014, 2018, 2020; Fedje et al., 2018).

METHODS

Sampling Protocols

Our literature search and material collection and processing methods have been described in Carlson (2007, 2012), Carlson and Baichtal (2015). and Lesnek et al. (2020). The multiple elevation datums used for this data set reflect what was reported by various authors over >120 years. For all of our newly acquired samples, elevation measurements were taken using handheld barometric digital altimeters accurate to ±1 m and that were zeroed as frequently as possible. Measured elevations are reported as meters above or below mean lower low water (AMLLW or BMLLW, respectively) or a 0.0 m tide. No attempt was made to change originally reported elevations or datums unless the site was revisited and the elevation measured to a 0.0 m tide. Many samples are reported simply as above sea level or above mean high tide (AMHT). For these samples, we do not know where the precise datum of the elevation measurement was taken. In practice, the measurement is commonly taken at the drift line or near the extreme high-tide line, which is not a precise datum. Across the study area, the elevation range in the modern high-tide line (HTL), the line of intersection of the land with the water's surface at the maximum height reached by a rising tide, varies substantially. The HTL ranges from 3.9 m AMLLW near Sitka, Alaska, to 6.4 m AMLLW near Haines, Alaska. For simplicity, all elevations not directly measured are reported here as above or below sea level as in the original publications. All directly measured elevations are reported as AMLLW or BMLLW. Lidar data collected in 2017 and 2018 for Prince of Wales, Annette, Gravina, Kuiu, and Kupreanof Islands and the islands west of Prince of Wales Island were delivered with a vertical datum of North American Vertical Datum of 1988 (NAVD88), geoid model GEOID12B, in meters (Alaska Division of Geologic and Geophysical Surveys elevation portal; https://elevation.alaska.gov/; accessed February 2021). Lidar data for the Haines vicinity collected in 2020 were also delivered with a vertical datum of NAVD88, GEOID12B, in meters (Daanen et al., 2021).

As stated in Lesnek et al. (2020), bulk samples of shell-bearing strata were collected in gallon-sized resealable plastic bags. Recovered samples were washed and screened through two graduated U.S.A. Standard Testing Sieves: #16, 1.18 mm (0.0469 inches); and #200, 0.075 mm (0.0029 inches). Care was taken to date charcoal or wood in addition to

shells whenever possible. When sampling charcoal or wood, individual conifer needles or small limbs were selected when possible to minimize possible "old wood" errors (Carlson, 2012). When dating shell material, short-lived species were favored over longer-lived species. If a large shell was the only datable material, only the outermost growth was used. At one site, described below, fish bones were recovered and sent for species-level identification (Carlson, 2007). Over 230 samples of shell-bearing strata are currently stored at the U.S. Forest Service Tongass National Forest in Thorne Bay, Alaska; the Museum of the North at the University of Alaska Fairbanks is the intended repository of these materials.

^{14}C Dating

Samples were prepared for accelerator mass spectrometry measurements at Beta Analytic, Miami, Florida, USA, or the U.S. Geological Survey ^{14}C Laboratory, Reston, Virginia, USA, and ^{14}C measurements were completed at Beta Analytic or Lawrence Livermore National Laboratory (Livermore, California, USA). The ages were calibrated in OxCal version 4.3 (Bronk Ramsey, 2009) using the IntCal20 (Reimer et al., 2020) and Marine20 (Heaton et al., 2020) calibration curves and locally derived marine reservoir corrections (Schmuck et al., 2021; see below). Calibrated ages are reported as the upper and lower limits of the entire calibrated age range at 2σ uncertainty.

Schmuck et al. (2021) aggregated shell-wood sample pairs from publications across the northwestern North American Pacific Coast to identify variation in the marine reservoir effect between samples of similar ages, with significant regional shifts in the reservoir effect through time. One of their most significant findings was the identification of a dramatic decrease in the reservoir age [$R(t)$] from the Bølling-Allerød interstade [$R(t)$ = 1100 ± 170 yr, ΔR = 575 ± 165] to roughly the global average in the Younger Dryas stade [$R(t)$ = ± 200 yr, ΔR = –55 ± 110]. A causal mechanism for this shift is provided by Praetorius et al. (2020), who argued for a persistent meltwater pulse (via the Columbia River) that freshened the North Pacific and lowered sea-surface temperature during the Younger Dryas. This freshening and stratification of surface waters corresponded with a shutdown of deep-water ventilation and decreased coastal upwelling, delivering less "old carbon" from the ocean basin to nearshore benthic communities during this period. The variability inherent in the marine reservoir effect, compounded by plateaus in the radiocarbon calibration curve during the Younger Dryas, unfortunately results in high uncertainty, but acknowledging this variability most faithfully represents confidence in our data set. With the return of coastal upwelling in the early Holocene, reservoir effects increased [$R(t)$ = 700 ± 195 yr, ΔR = 245 ± 200] before stabilizing for much of the Holocene [between ca. 9000 and 2000 cal. yr B.P.; $R(t)$ = 665 ± 135 yr, ΔR = 145 ± 165]. In southeastern Alaska, early and mid-Holocene values are slightly higher [$R(t)$ = 700 ± 195 yr, ΔR = 265 ± 205; and $R(t)$ = 750 ± 170 yr, ΔR = 225 ± 185, respectively] likely due to the "hard water effect" of local karst systems. By the late Holocene (between 2000 cal. yr B.P. and 200 cal. yr B.P.), the reservoir correction decreased further [$R(t)$ = 630 ± 110, ΔR = 140 ± 100] (Schmuck et al., 2021).

RESULTS AND SITE-SPECIFIC INTERPRETATIONS

A total of 436 ^{14}C ages from 723 samples of shell-bearing strata across southeastern Alaska (Fig. 2) provide constraints on postglacial sea-level change (Table S1 in the Supplemental Material[1]). The dated material comes from a variety of elevations, ranging from 430 m below sea level to 191 m above sea level. We use these ages from shell-bearing strata in conjunction with ^{14}C ages from marine sediment cores and other terrestrial deposits to develop relative sea-level curves for 11 zones within southeastern Alaska (Figs. 3A–3K). Our description of these zones is generally structured to take the reader from the areas of least uplift to those of greatest uplift. We interpret the disparity in postglacial uplift between these zones as crustal response due to variable ice loading and unloading, with the greatest ice loading occurring at the Juneau mainland and northern Admiralty Island. We provide relative sea-level curves for each of these zones based on the chronology presented here and the elevations of beach ridges apparent on lidar bare-earth models (Figs. 3A–3K).

The oldest dated sites that overlap at 2σ in all 11 zones range in age from 14,870 ± 630 to 12,820 ± 340 cal. yr B.P. (Fig. 4). Our relative sea-level curves are further constrained by paleoshorelines that were mapped from lidar digital terrain models, which, in the absence of ^{14}C-dated shell material, have in some cases been used to define the maximum elevation of postglacial transgression. Below, we describe the chronology from each of the 11 zones, including ^{14}C ages from both shell and charcoal samples.

Baranof and Kruzof Islands (11 Samples)

In the vicinity of Sitka Sound, shell-bearing strata can be found in inland stream banks and modern upper intertidal sediments. ^{14}C ages from these sites range from 7930 ± 390 to 1940 ± 480 cal. yr B.P.; ages on the four oldest deposits overlap within 2σ uncertainty and range from 7930 ± 390 to 7630 ± 90 cal. yr B.P. In this zone, the highest shell occurrence documented to date lies at 4.0 m AMLLW (Fig. 4). Storm berm surge deposits exposed where power poles have been placed at an elevation of 9.0 m AMLLW record the maximum marine transgression in the Sitka area; however, these deposits are not dated at this time (Fig. 5D).

Prince of Wales Island and the Islands to the West (172 Samples)

By far the highest density of shell-bearing strata we report is from Prince of Wales Island and the islands to the west. Numerous shell beds can be found in inland stream banks, beneath wetlands, and from upper intertidal sediments (Figs. 5 and 6). These deposits have been located by field reconnaissance, and exposed by road construction, quarry development, and excavation. These range in age from 11,995 ± 415 to 40 ± 40 cal. yr B.P. (Table S1 [footnote 1]). The oldest dated deposits within 2σ uncertainty range in age from 11,000 ± 390

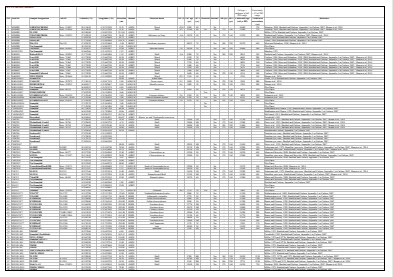

[1]Supplemental Material. Shell-bearing strata dataset from southeastern Alaska. Please visit https://doi.org/10.1130/GEOS.S.15121974 to access the supplemental material, and contact editing@geosociety.org with any questions.

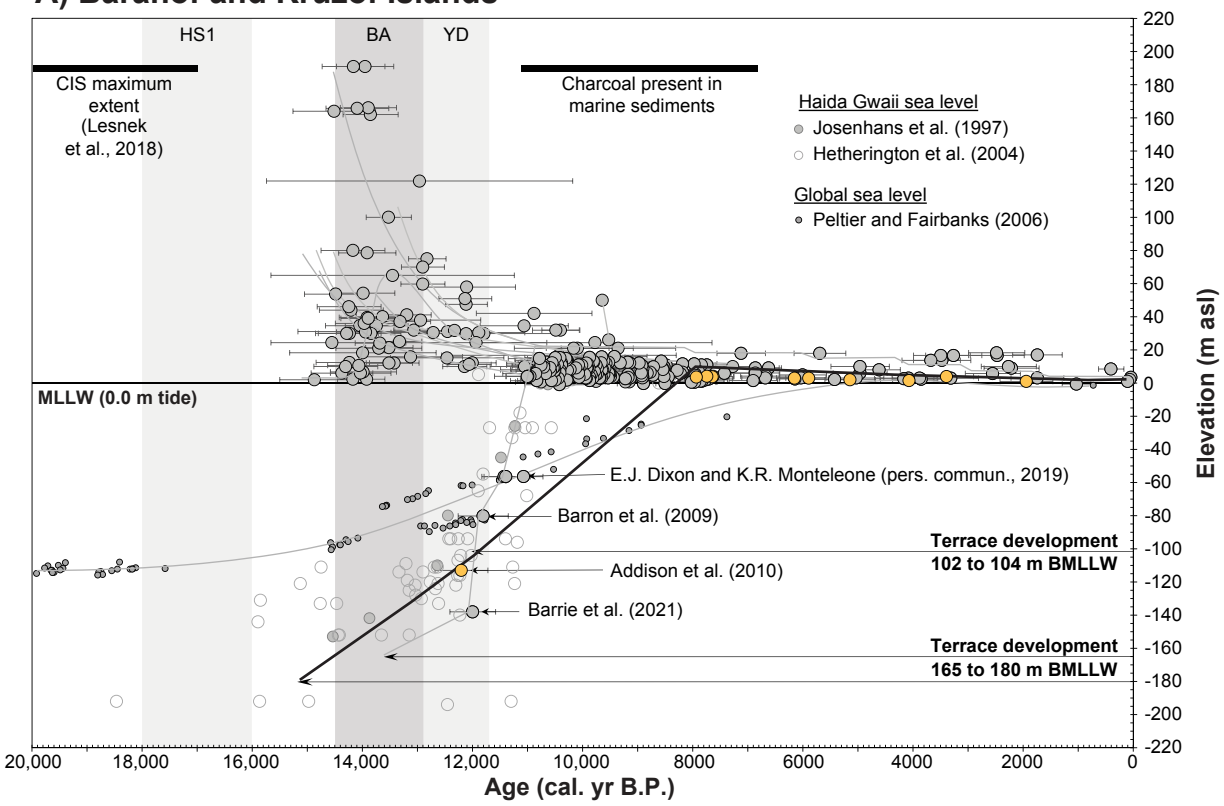

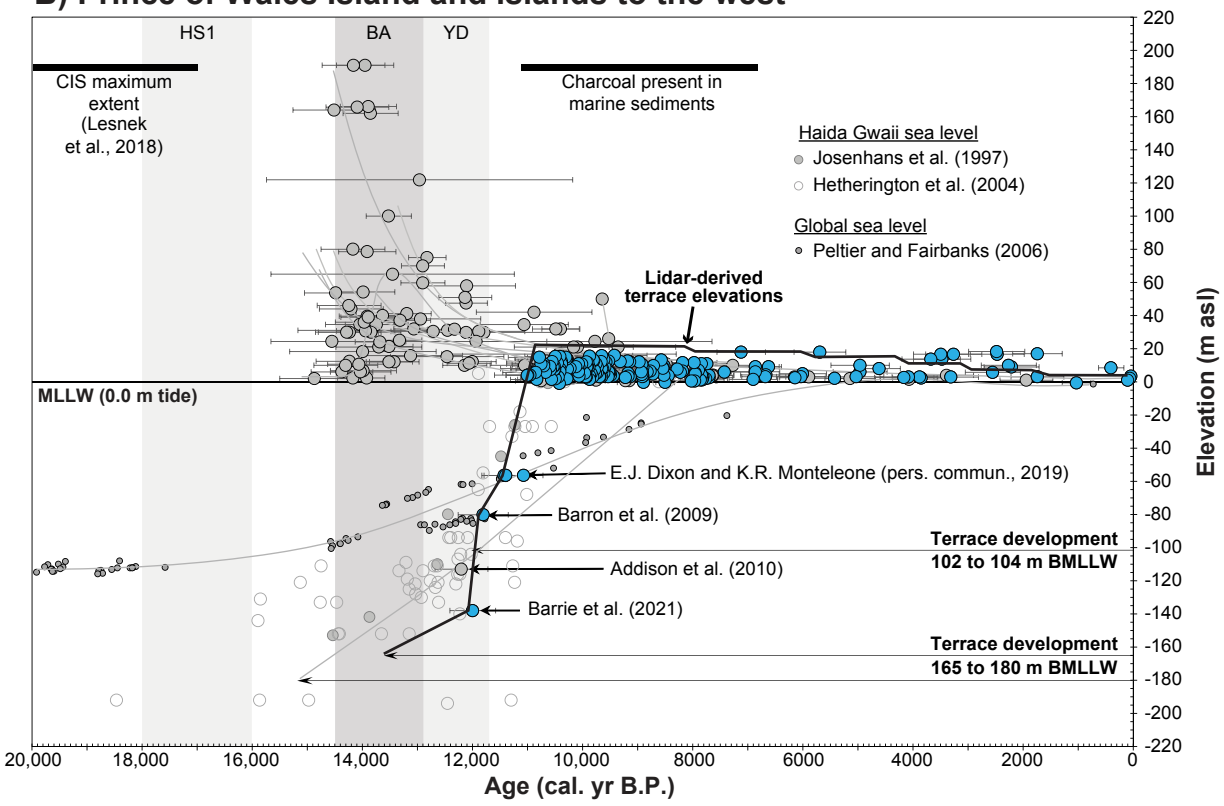

Figure 3. (*Continued on following 5 pages.*)

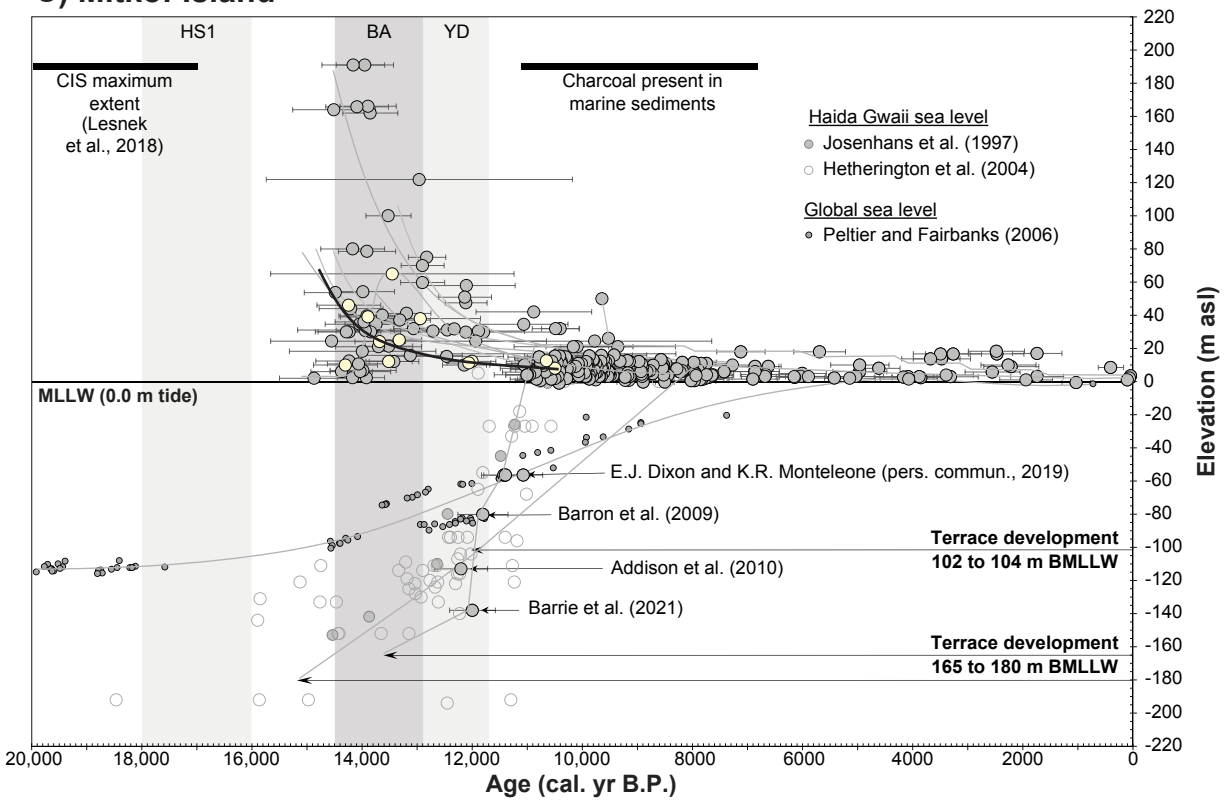

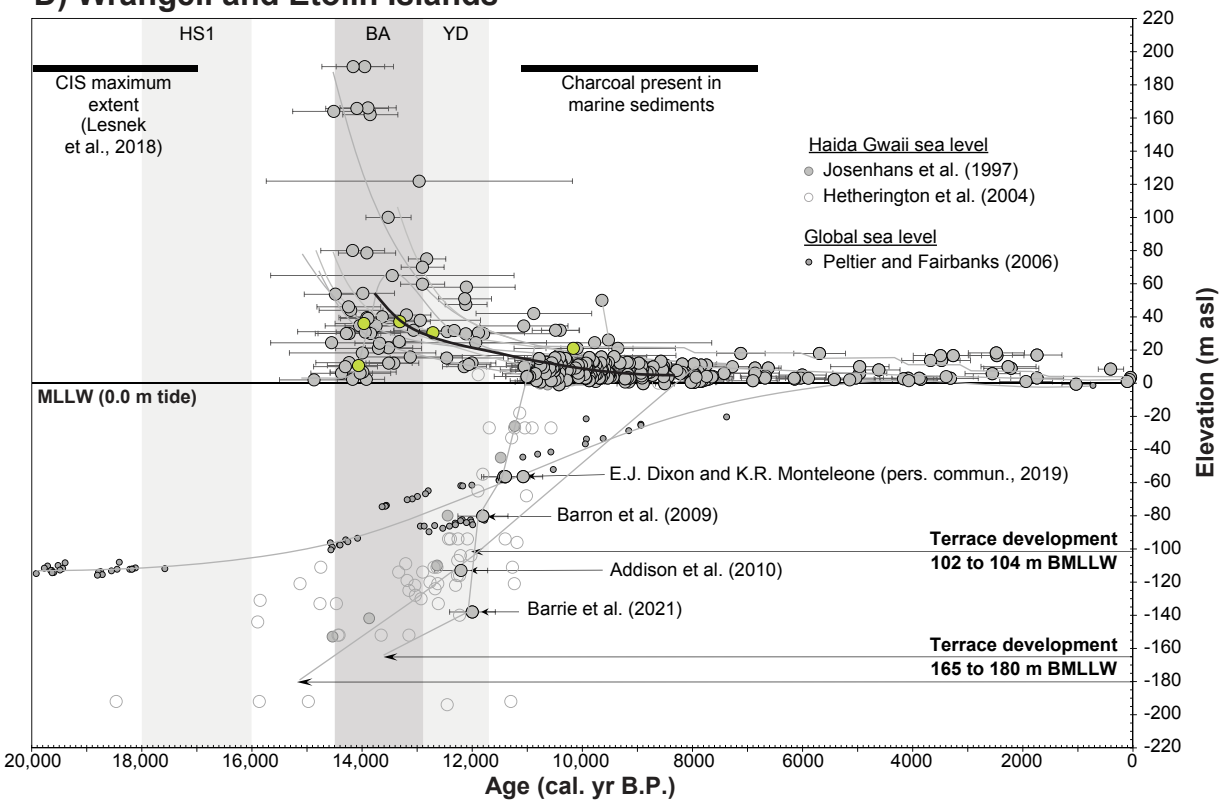

Figure 3. (***Continued on following 4 pages.***)

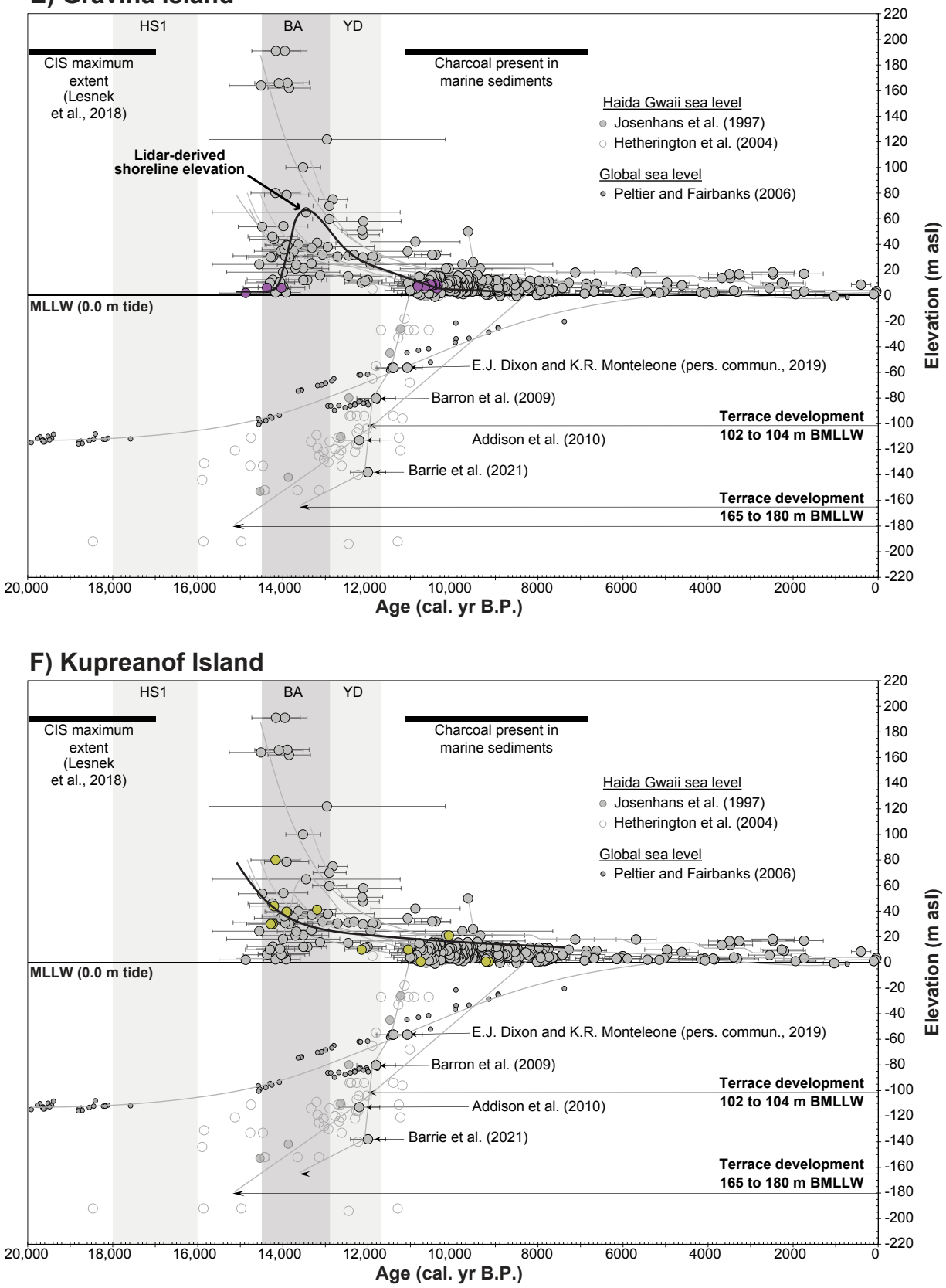

Figure 3. (*Continued on following 3 pages.*)

G) Revillagigedo Island

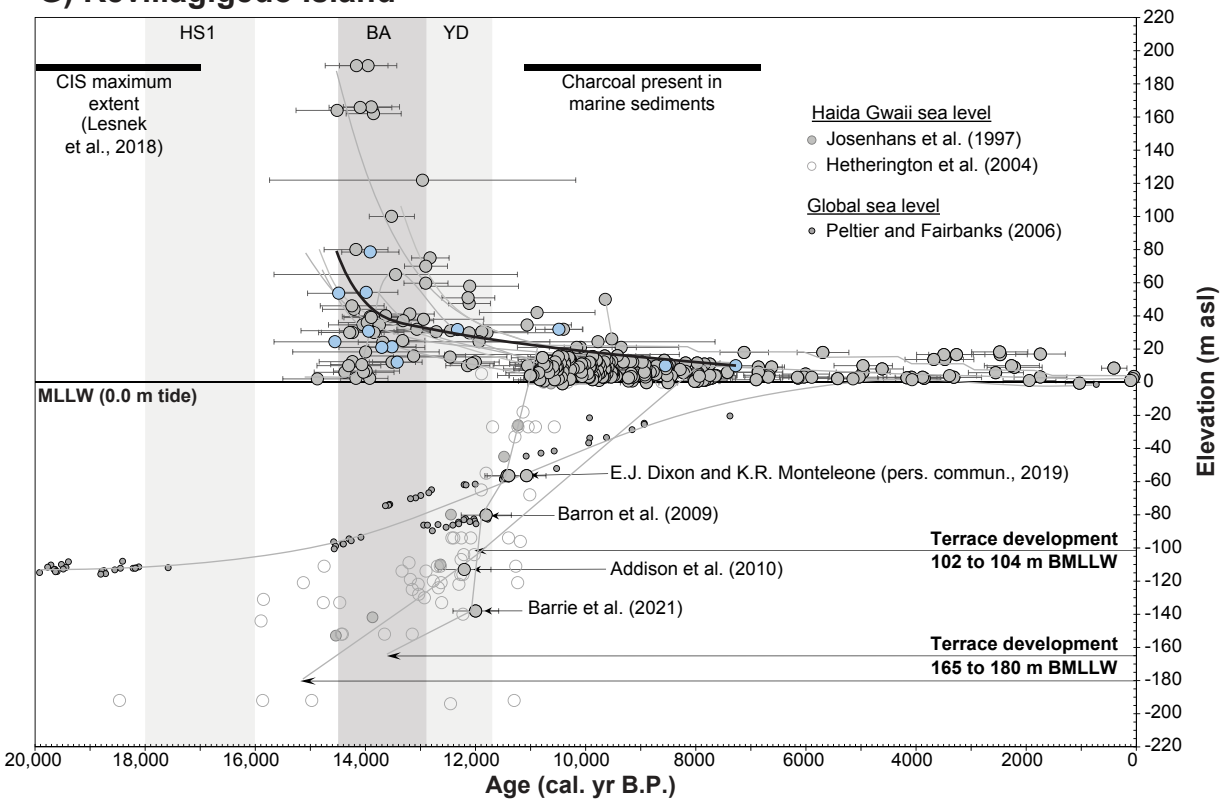

H) Chichagof Island

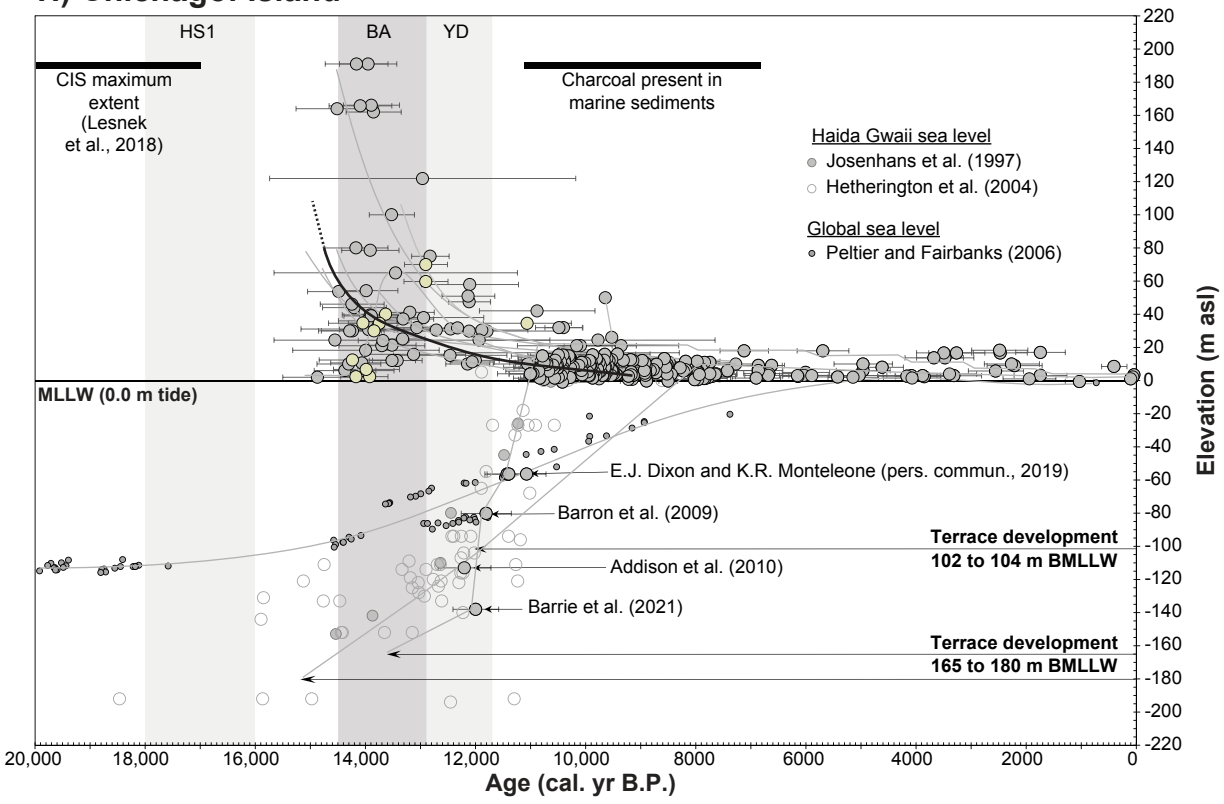

Figure 3. (*Continued on following 2 pages.*)

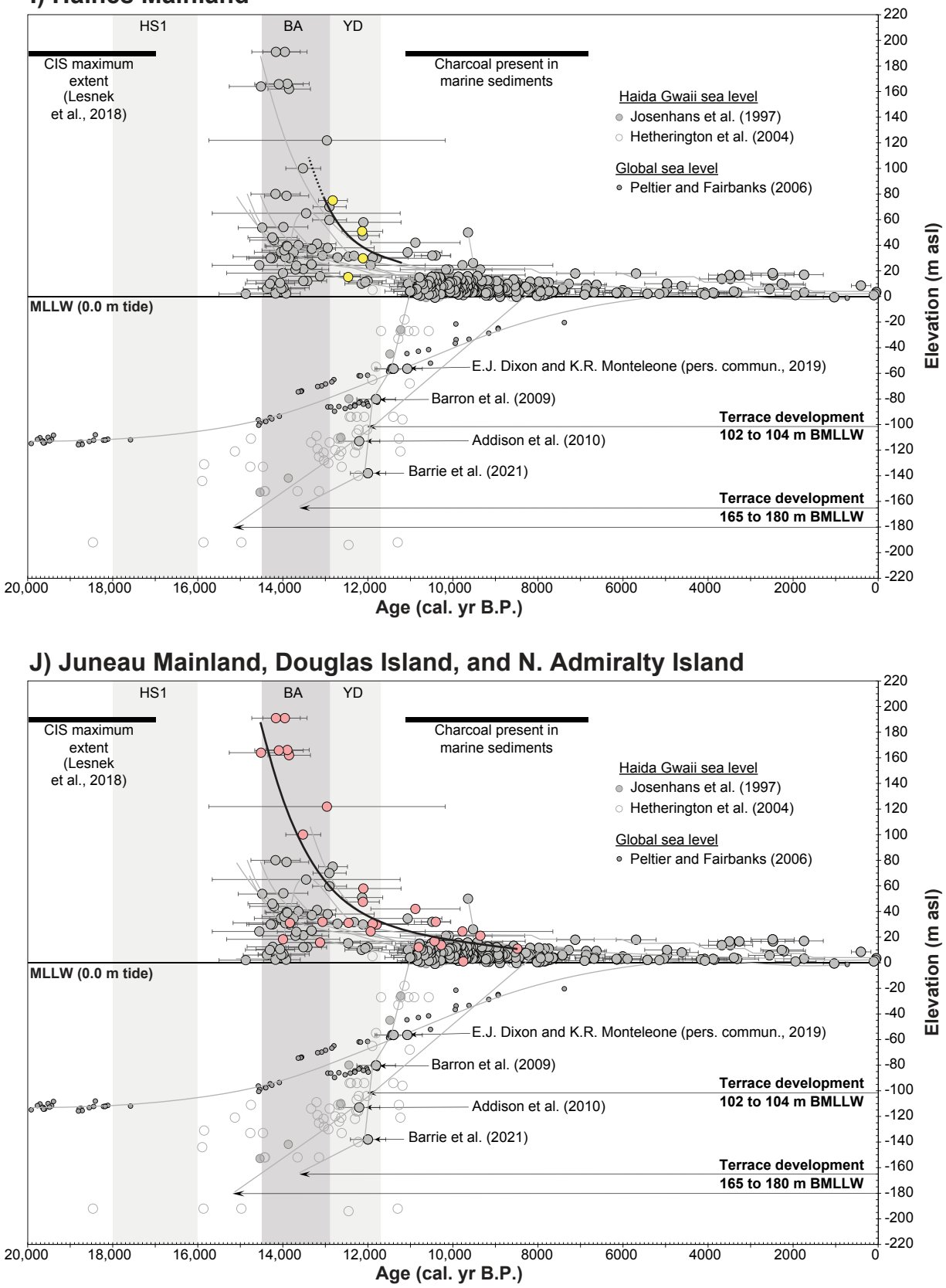

Figure 3. (*Continued on following page.*)

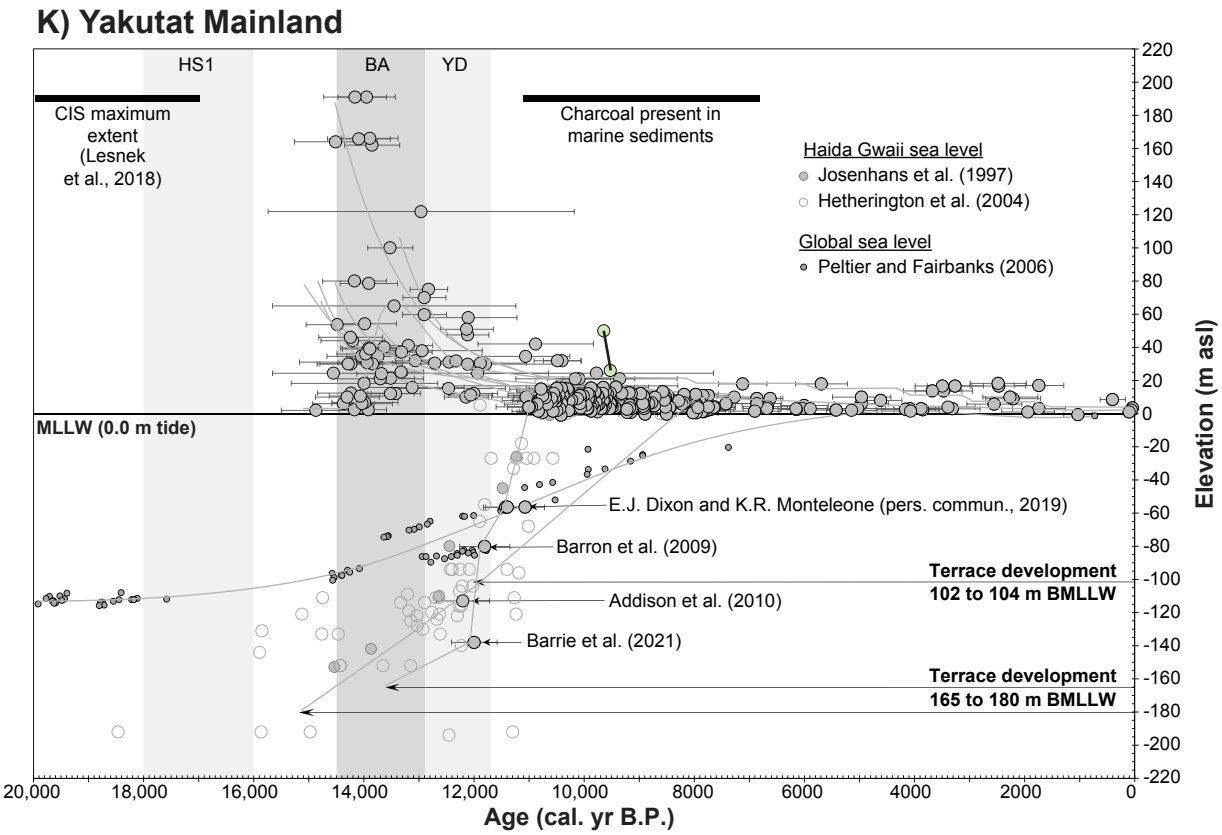

Figure 3. Updated sea-level curves for southeastern Alaska with Haida Gwaii (British Columbia, Canada) data (gray and white circles; Josenhans et al., 1997; Hetherington et al., 2004) and global sea level (small gray circles; Peltier and Fairbanks, 2006). Each panel highlights the ^{14}C ages (colored dots) and relative sea-level curve (thick black line) for a single analysis zone. Dotted lines indicate extrapolations of the relative sea-level curves. Each panel also shows the ^{14}C ages (gray circles) and relative sea-level curves (thick gray lines) for all analysis zones for ease of comparison between sites. Plots show elevation versus age of the shell-bearing strata from 11 analysis zones across the study area. Zones may encompass several islands or a single island. Sea-level curves for each zone define the timing of the relative sea-level change over the past 14,000 yr following the retreat of the Cordilleran Ice Sheet (CIS). The data points for each zone are color coded to match the analysis zone extents in Figure 2. Error bars indicate 2σ uncertainty for each calibrated ^{14}C age. The sea-level curve for Prince of Wales Island and the western islands (southern Kuiu, Kosciusko, Heceta, Tuxekan, Noyes, and Suemez Islands) was partially derived from lidar interpretation. The sea-level curves for Gravina Island and Haines mainland also reflect shorelines interpreted from lidar. We include marine sediment core data from Josenhans et al. (1997) and Hetherington et al. (2004) for reference. We also show the global sea-level curve as defined by Peltier and Fairbanks (2006). HS1— Heinrich Stadial 1; BA—Bølling-Allerød; YD—Younger Dryas; MLLW—mean lower low water; BMLLW—below mean lower low water; cal.—calibrated.

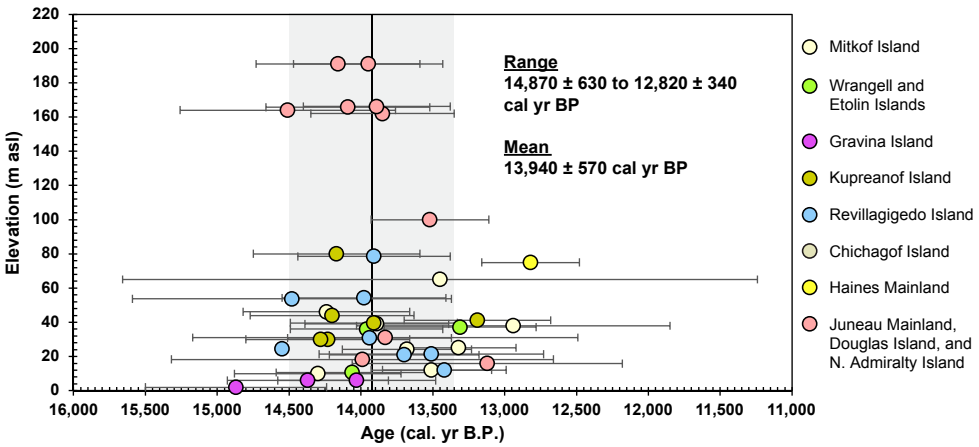

Figure 4. Minimum-limiting age constraints on Cordilleran Ice Sheet deglaciation. The oldest dated sites that overlap at 2σ from the eight zones farthest from the western shores (listed at right) range in age from 14,870 ± 630 to 12,820 ± 340 cal. yr B.P. Data points are color coded to correspond to the zones shown in Figure 2. Vertical gray bars represent the mean and 1σ uncertainty of the ^{14}C ages.

Figure 5. Examples of shell-bearing strata from across the study area. (A) Shell-bearing strata from Bostwick Creek at the head of Bostwick Bay on Gravina Island, Alaska. Samples GRAVINA8 and GRAVINA9 at 9.0 m above mean lower low water (AMLLW) date to 10,120 ± 580 calibrated yr B.P. and 10,420 ± 140 cal. yr B.P., respectively. The site contains not only a record of the intertidal molluscan fauna, but also wood, cones, seeds, and elements washed in from the surrounding landscape. The scales and vertebra of Pacific sardine (*Sardinops sagax*) were recovered from these samples. Scale bar is 10 cm. (B) Shell-bearing strata from Cape Pole, Kosciusko Island, Alaska. Sample KOS8 at 13.48 m AMLLW dates to 9610 ± 550 cal. yr B.P. (C) Shell-bearing strata in DeGroff Bay on Krestof Island west of Sitka, Alaska. These deposits have been dated to 7630 ± 50 cal. yr B.P. (D) Storm berm surge deposits exposed where power poles have been placed at an elevation of 9.0 m AMLLW. This records the maximum marine transgression in the Sitka area, although the deposit is undated. White bar in panels C and D are ~10 cm.

to 10,500 ± 420 cal. yr B.P. (17 samples) (Fig. 7). The highest shell occurrence is 18 m AMLLW. Lidar data acquired in 2017 and 2018 clearly show an average of six eroded shorelines, with the upper shoreline or terrace ranging from 19 to 25 m asl (Alaska Division of Geologic and Geophysical Surveys, elevation portal; https://elevation.alaska.gov/) (Fig. 8).

Mitkof Island (12 Samples)

Numerous shell-bearing strata have been reported from Mitkof Island by Yehle (1978) and Viens (2001). Many of these original sites have been relocated, had their elevations carefully measured, and been resampled. These shell beds are exposed in stream and river banks, cut banks, and ditches associated with road construction, landslides, and excavations. Mitkof Island dates range from 14,300 ± 580 to 10,490 ± 1000 cal. yr B.P., and the sites range in elevation from 5.5 to 72.0 m asl. The highest reported elevation of shell-bearing strata lies beneath the Petersburg Solid Waste Baler Facility at ~72 m asl. During construction, it was reported that shell-bearing diamicton was excavated into and the facility built over it. No sample of this material has been recovered for analysis. The oldest dated deposits within 2σ uncertainty range in age from 14,300 ± 580 to 12,490 ± 1090 cal. yr B.P. (eight samples).

Wrangell and Etolin Islands (8 Samples)

Numerous shell-bearing strata have been reported from Wrangell and Etolin Islands by Lemke (1974). Many of these original sites have been relocated, had their elevations carefully measured, and been resampled. These shell beds are exposed in stream and river banks, cut banks, and ditches associated with road construction, landslides, and excavations. Wrangell and Etolin Islands dates range from 14,060 ± 570 to 10,160 ± 1080 cal. yr B.P., and the sites range in elevation from 10.6 to 40.0 m asl. The oldest dated deposits within 2σ uncertainty range in age from 14,060 ± 570 to 13,310 ± 550 cal. yr B.P. (three samples).

Gravina Island (14 Samples)

Most of the confirmed shell-bearing strata on Gravina Island came from Bostwick Inlet and Seal Cove on the central-southern shore of the island. The two oldest sites consist of very hard, compacted, shell-bearing diamicton that contain abundant diatoms. The sample contains well-preserved sea-ice marine diatoms and marginal sea-ice diatoms including *Fragilariopsis cylindrus*, *Thalassiosira nordenskioeldii*, *Thalassiosira antarctica*, *Thalassiosira hyalina*, and *Porosira glacialis* (J.A. Barron, 2017, personal commun.). Gravina Island dates range from 14,870 ± 630 to 9180 ± 560 cal. yr B.P., and the sites range in elevation from 5.5 to 9.0 m AMLLW (Fig. 5A). The oldest dated deposits within 2σ uncertainty range in age from 14,870 ± 630 to 14,030 ± 550 cal. yr B.P. (three samples). Geomorphic interpretation of lidar digital terrain models acquired in 2018 has identified eight wave-eroded shorelines from 6.0 m to 76.0 m asl (Alaska Division of Geologic and Geophysical Surveys elevation portal; https://elevation.alaska.gov/). This likely represents the highest stand of postglacial sea level (Fig. 9).

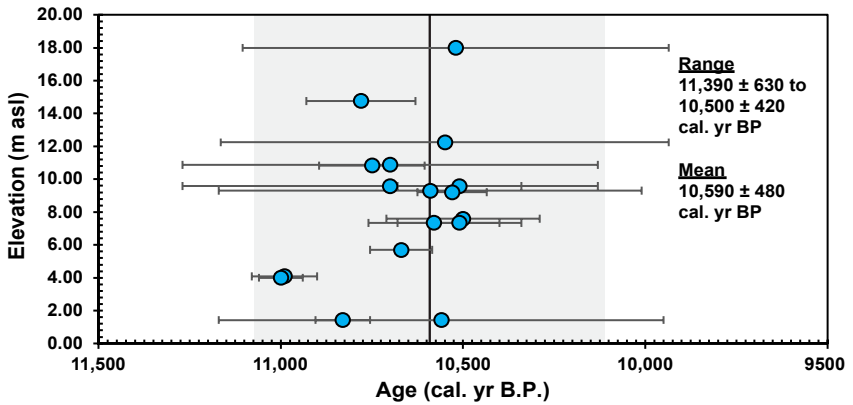

Figure 6. Examples of shell-bearing strata from across the study area. (A) The highest dated occurrence of shell-bearing strata in the study area at 191.0 m above mean high tide at Spaulding Meadows, Auke Bay, Alaska. Two samples from this site, JUNEAU23 and JUNEAU68, date to 13,950 ± 520 calibrated yr B.P. and 14,060 ± 570 cal. yr B.P., respectively. These samples lie beneath the Mount Edgecumbe dacite tephra (MEd), which dates to 13,165 ± 85 cal. yr B.P. (Riehle et al., 1992a, 1992b; Begét and Motyka, 1998; Baichtal, 2014). (B) Shell-bearing strata from Noyes Island, Alaska; sample NOYES4 at 5.9 m above mean lower low water (AMLLW) dates to 8910 ± 520 cal. yr B.P. (C) Shell-bearing strata from Irish Creek, Kupreanof Island, Alaska; sample KUPRE7 at 0.6 m AMLLW dates to 10,750 ± 240 cal. yr B.P. (D) Shell-bearing strata from Kassa Inlet, Prince of Wales Island, Alaska; sample POW220 at 3.5 m AMLLW dates to 8900 ± 120 cal. yr B.P. White bar in each panel is ~10 cm.

Kupreanof Island (14 Samples)

Many shell-bearing sites have been reported from Kupreanof Island. These shell beds are exposed in stream and river banks, cut banks, and ditches associated with road construction and excavations. Kupreanof Island dates range from 14,280 ± 570 to 9150 ± 560 cal. yr B.P., and the sites range in elevation from 0.6 to 80.0 m asl. The oldest dated deposits within 2σ uncertainty range in age from 14,280 ± 570 to 13,910 ± 510 cal. yr B.P. (five samples). In 2018, high-resolution lidar data were acquired for some of Kupreanof Island near Kake. Geomorphic interpretation of lidar data acquired in 2018 has identified 18 possible shorelines from 4.5 m to 102.5 m asl (Alaska Division of Geologic and Geophysical Surveys elevation portal; https://elevation.alaska.gov/) (Fig. 10). The highest known

Figure 7. Minimum-limiting transgression date for the Prince of Wales Island and western islands zone, which includes southwestern Kuiu, Heceta, Kosciusko, and western Prince of Wales Islands. Error bars indicate 2σ uncertainty for each calibrated ^{14}C age. We interpret the age of the oldest deposits across this portion of the study area as the minimum-limiting age for the transgression associated with the collapse of the forebulge. Vertical gray bars represent the mean and 1σ uncertainty of the ^{14}C ages.

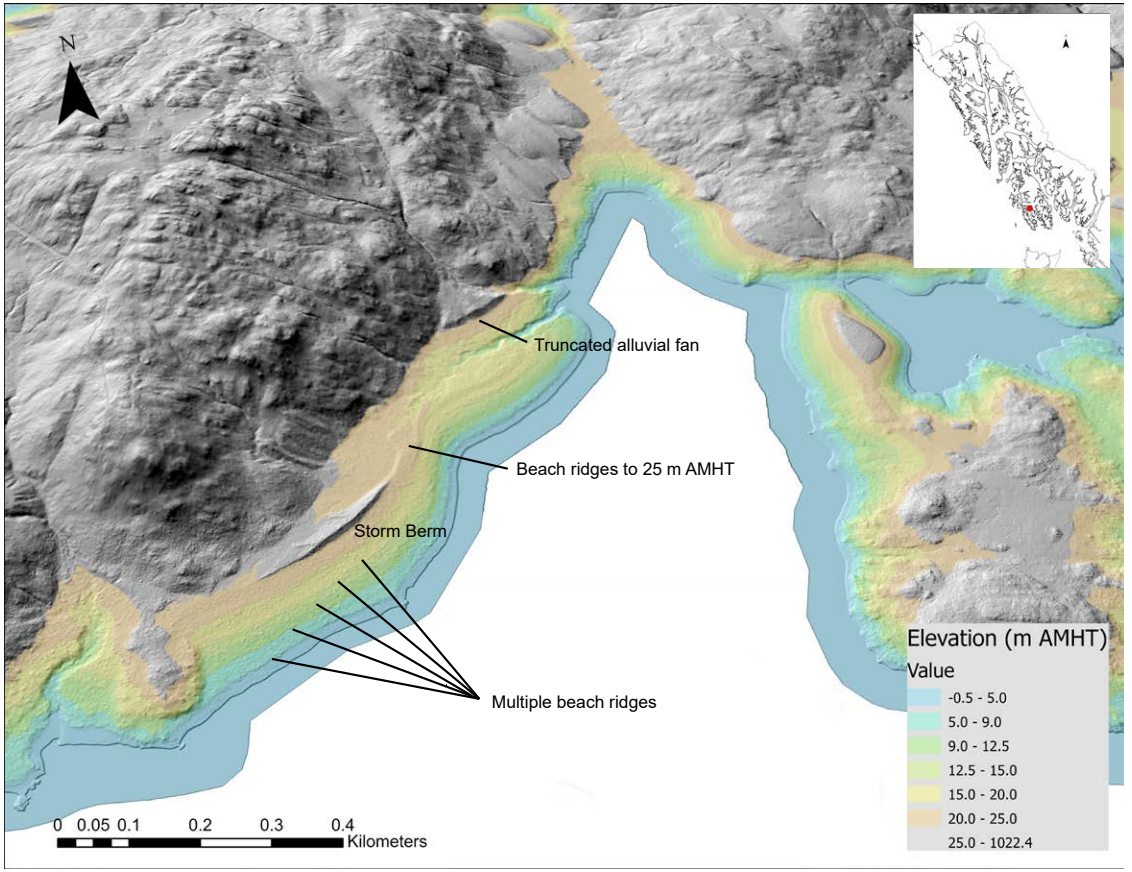

Figure 8. Example of the shorelines apparent in the acquired 2017 and 2018 lidar data (Alaska Division of Geologic and Geophysical Surveys elevation portal; https://elevation.alaska.gov/). The image is from a portion of Prince of Wales Island 9.5 km west of Hydaburg, Alaska, near a peninsula named Halibut Nose. The center of the image is approximately at 55.21936°N, 132.97480°W. Multiple beach ridges are visible up to 25 m above mean high tide (AMHT). Storm berms and a truncated fluvial fan edge clearly define the maximum marine transgression between 11,000 ± 390 and 10,500 ± 420 calibrated yr B.P.

shell occurrence sits in deep glacial clays exposed during road construction beneath the highest interpreted shoreline.

Revillagigedo Island (28 Samples)

Numerous shell-bearing strata have been reported from Revillagigedo Island by Stuckenrath (1971) and Lemke (1975). Many of these original sites have been relocated, had their elevations carefully measured, and been resampled. These shell beds are exposed in stream and river banks, cut banks, and ditches associated with road construction, landslides, and excavations. Revillagigedo Island dates range from 14,550 ± 1110 to 7270 ± 470 cal. yr B.P., and the sites range in elevation from 10.0 to 85.0 m AMLLW. Wave-cut notches and terraces can be found in several places from 80 to 85 m asl. The oldest dated deposits within 2σ uncertainty range in age from 14,550 ± 1110 to 13,510 ± 430 cal. yr B.P. (seven samples).

Chichagof Island (19 Samples)

Many shell-bearing sites have been reported from Chichagof Island. These shell beds are exposed in stream and river banks, cut banks, and ditches associated with road construction and excavations. Chichagof Island shell-bearing strata dates range from 14,230 ± 610 to 11,060 ± 800 cal. yr B.P., and the sites range in elevation from –4.7 to 60.0 m asl. In 2014, high-resolution lidar data were acquired on northeastern Chichagof Island near Hoonah. Geomorphic interpretation has identified a terrace eroded into glacial features and landslide deposits at 107 m asl (Alaska Division of Geologic and Geophysical Surveys elevation portal; https://elevation.alaska.gov/) (Fig. 11). This likely represents the highest stand of postglacial sea level.

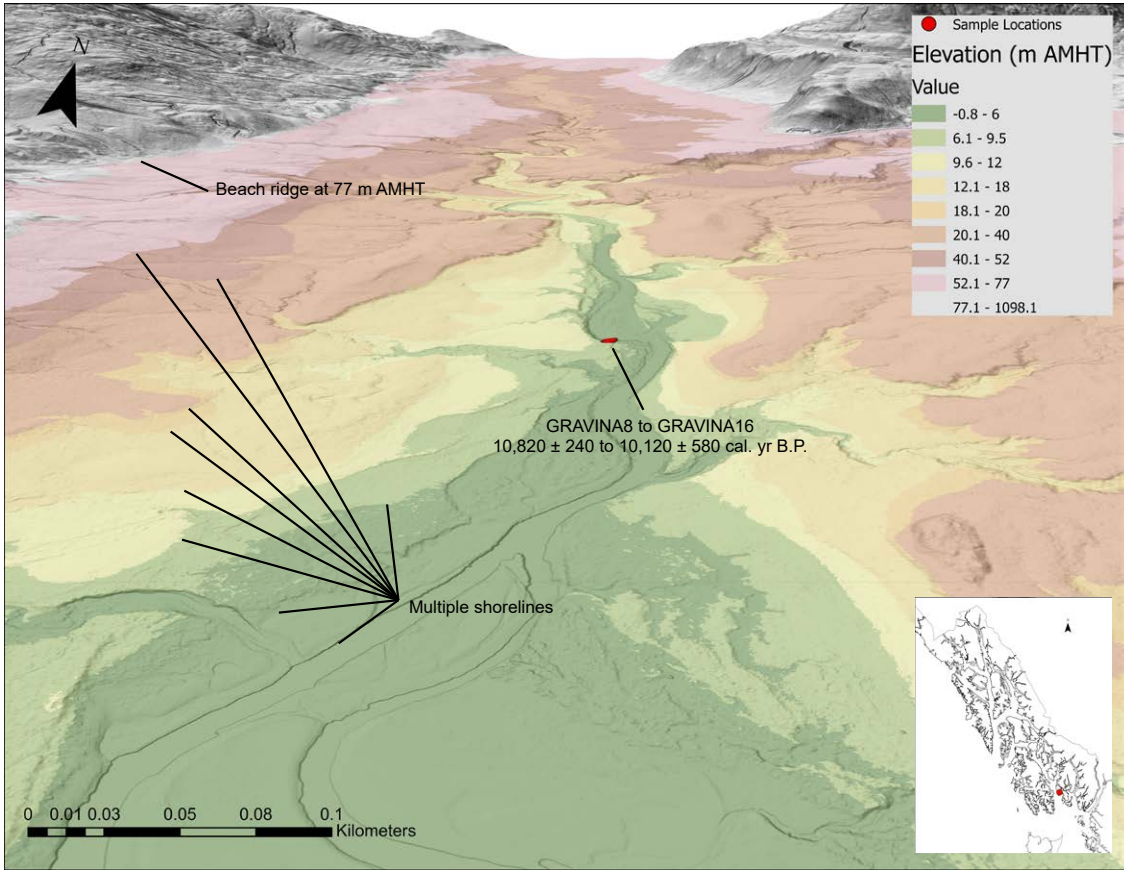

Figure 9. Example of the shorelines interpreted from lidar data acquired in 2018 (Alaska Division of Geologic and Geophysical Surveys elevation portal; https://elevation.alaska.gov/) on Gravina Island. The center of the image is approximately at 55.261069°N, 131.769609°W. The lidar data show at least eight storm berms and wave-eroded shorelines up to 77 m above sea level (Alaska Division of Geologic and Geophysical Surveys elevation portal; https://elevation.alaska.gov/). Breaks in the color scheme show the elevation of these berms and shorelines. The location of samples GRAVINA8 through GRAVINA16 dating from 10,820 ± 240 to 10,120 ± 580 calibrated yr B.P. is shown. Pacific sardine (*Sardinops sagax*) remains were recovered from the uppermost beds of this location. AMHT—above mean high tide.

Haines Mainland (4 Samples)

Several shell-bearing strata have been reported near Haines, on the Alaska mainland, by Lemke and Yehle (1972a). In 2020, the highest and oldest shell-bearing diamicton in the vicinity of Haines was discovered (J.P. Norton, 2020, personal commun.) at an elevation of 75.0 m asl. Shell-bearing strata in the vicinity of Haines range in age from 12,820 ± 340 to 12,110 ± 380 cal. yr B.P., and the sites range in elevation from 6.1 to 75.0 m asl. Lidar digital terrain models acquired in 2014 and 2020 show at least 26 storm berms and wave-eroded shorelines up to 107 m asl (Alaska Division of Geologic and Geophysical Surveys elevation portal; https://elevation.alaska.gov/) (Fig. 12). This likely represents the highest elevation of postglacial sea level.

Juneau Mainland, Douglas Island, and Northern Admiralty Island (27 Samples)

The Juneau and Douglas Island vicinities are the type locality for the Gastineau Channel Formation, first described by R.D. Miller in 1973 (Miller, 1973b) and mapped in 1975 (Miller, 1975). The highest-elevation marine diamicton is recorded from Montana Creek (Miller 1973b, 1975) at 229 m asl. No shell was described from this site, and the dated material was an upper limiting date from basal peat above the diamicton. The highest record of shell-bearing diamicton is on northern Admiralty Island at 212 m asl (Miller, 1973a). No sample is available from this site. The highest dated sample comes from Spaulding Meadows above Auke Lake north of Juneau at 191 m asl (Fig. 6A). The oldest sample taken from this site dates to 14,160 ± 570 cal. yr B.P. The oldest dated sample was recovered from Douglas Island on Fish Creek at an elevation of 164 m AMLLW, with an age of 14,510 ± 750 cal. yr B.P. Both of these

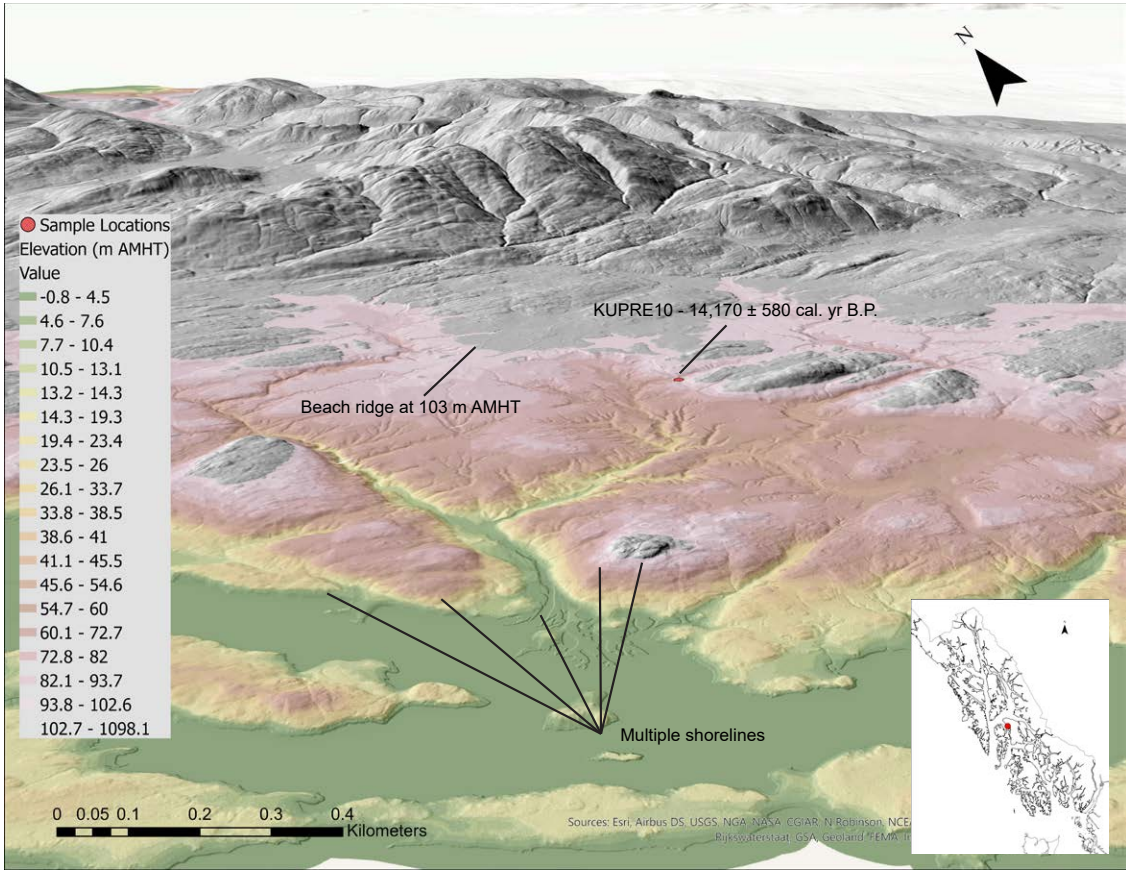

Figure 10. Example of the shorelines interpreted from lidar data acquired in 2018 (Alaska Division of Geologic and Geophysical Surveys elevation portal; https://elevation.alaska.gov/) near Kake, Alaska, on northwestern Kupreanof Island. The center of the image is approximately at 56.931270°N, 133.868172°W. The lidar data show at least 18 storm berms and wave-eroded shorelines up to 107 m above sea level (Alaska Division of Geologic and Geophysical Surveys elevation portal; https://elevation.alaska.gov/). Breaks in the color scheme show the elevation of these berms and shorelines. Sample KUPRE10 sits just below this highest interpreted shoreline. A *Saxidomus gigantea* shell at this site is dated to 14,170 ± 580 calibrated yr B.P. AMHT—above mean high tide.

samples are overlain by the Mount Edgecumbe dacite tephra, which dates to 13,160 ± 90 cal. yr B.P. (Begét and Motyka, 1998).

Yakutat Mainland (4 Samples)

The Yakutat forelands lie to the west of the Fairweather fault, an extension of the Queen Charlotte fault. Shell-bearing strata in the vicinity of Yakutat, on the Alaska mainland, range in age from 10,050 ± 600 to 1510 ± 620 cal. yr B.P., and the sites range in elevation from 26.0 to 50.0 m asl. Shell fragments taken from the push moraine enclosing Harlequin Lake at an elevation of 26 m asl date to 9520 ± 570 cal. yr B.P. Shell fragments taken from the area at an estimated elevation of 50 m in 1974 from similar moraine deposits were dated to 9640 ± 1080 cal. yr B.P. (Yehle, 1979). These deposits suggest that the Harlequin fjord persisted to at least 9640 ± 1080 cal. yr B.P., and likely much longer. At that time, the Yakutat Glacier may have been a tidewater glacier. The clams that now exist as shell fragments in the moraine lived in the intertidal portions of the fjord. It is believed that the late Holocene advance of the Yakutat Glacier began ca. 3000 yr ago, culminating at ca. 1850 CE at the southern end of Harlequin Lake (Barclay et al., 2001). Harlequin Lake as we know it began forming by 1903 (Trüssel et al., 2013). The Little Ice Age advance that created the moraine at the end of Harlequin Lake dug up the older marine sediments, incorporating them into the moraine. The Little Ice Age sediments from the Yakutat Glacier infilled the fjord, and the Dangerous River now flows on top of those sediments.

Charcoal and Pacific Sardine Occurrences in Shell-Bearing Strata

Charcoal was recovered from shell-bearing marine deposits from 40 sites and 99 samples

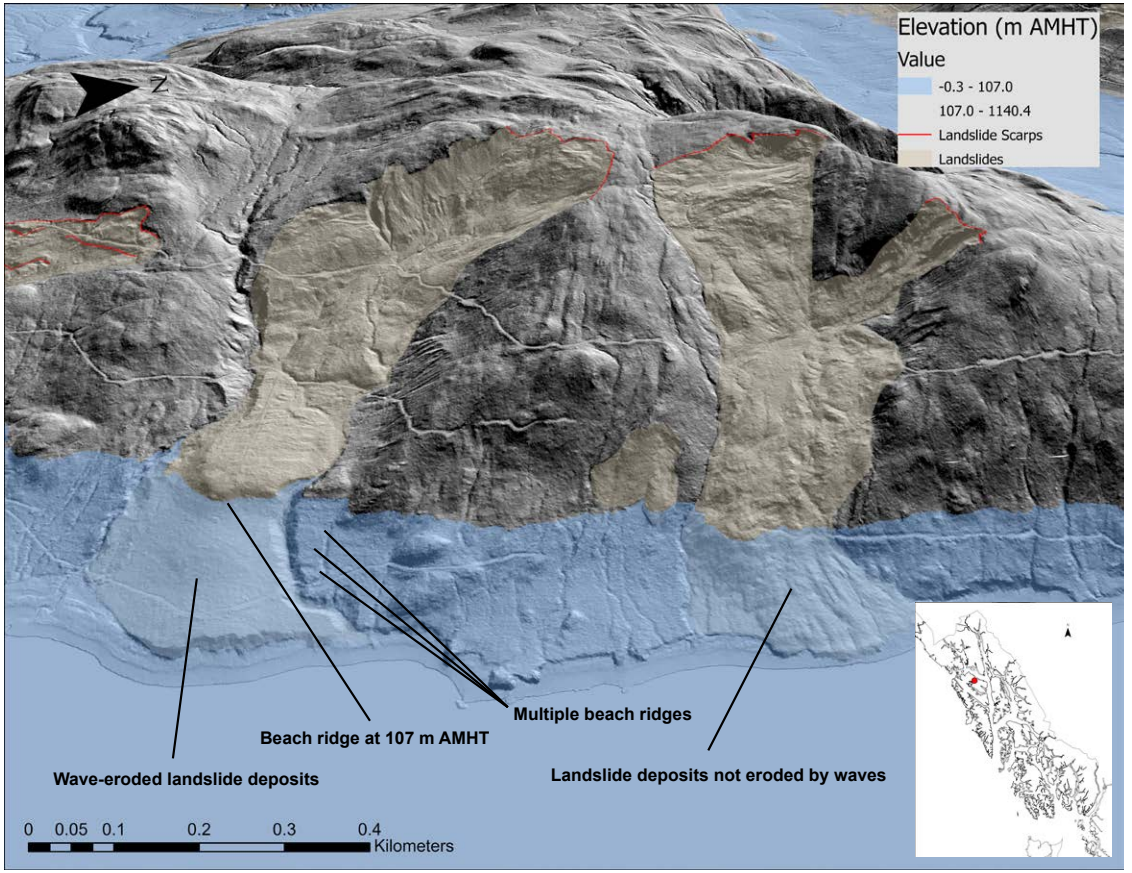

Figure 11. Example of the shorelines interpreted from lidar data acquired in 2015 (Alaska Division of Geologic and Geophysical Surveys elevation portal; https://elevation.alaska.gov/) near Hoonah, Alaska, on northeastern Chichagof Island. The center of the image is approximately at 58.126536°N, 135.525381°W. The highest clear geomorphic expression of a paleoshoreline from lidar interpretation is terraces eroded into landslide deposits on the western shore of Port Frederick. The southernmost landslide must have occurred prior to the sea-level rise that occurred from 14,870 ± 630 to 12,820 ± 340 calibrated yr B.P. A terrace is clearly eroded into these landslide deposits at an elevation of 107 m above mean high tide (AMHT), below which the landslide surfaces are eroded by wave action. The northern landslide shows no such erosion nor terrace development, suggesting the slope failure occurred after the maximum transgression.

ranging in age from 11,000 ± 390 to 3400 ± 110 cal. yr B.P. Charcoal dating to between ca. 11,000 and 7630 cal. yr B.P. is particularly abundant (Fig. 13). Though five sites younger than ca. 7630 cal. yr B.P. do contain charcoal, most sites younger than this do not contain charcoal. No charcoal was recovered from sites predating ca. 11,000 cal. yr B.P. At two sites, Yatuk Creek on Prince of Wales Island and Bostwick Creek on Gravina Island, Pacific sardine (*Sardinops sagax*) bones were found in charcoal deposits ranging in age from 10,780 ± 570 to 9870 ± 640 cal. yr B.P. (Figs. 13 and 14).

DISCUSSION

Pleistocene Sea Levels, Timing of Deglaciation, and Isostatic Response to Ice Loading and Unloading

Previously published ^{10}Be exposure ages from across the southern part of southeastern Alaska and coastal British Columbia provide direct constraints on the timing of CIS retreat between ca. 17,000 and 15,000 yr ago (Darvill et al., 2018; Lesnek et al., 2018, 2020). The dated materials from shell-bearing marine deposits throughout the study area provide minimum-limiting constraints on CIS deglaciation and the timing of the marine transgression as the result of forebulge collapse along the western margin of southeastern Alaska. When interpreted together, these two data sets reveal a consistent pattern of ice-margin change and sea-level fluctuations in the region.

Beginning possibly as early as 18,000 cal. yr B.P., but likely well under way by 17,000 cal. yr B.P., local sea levels rapidly rose, flooding fjords and straits and causing rapid calving of the CIS ice within them. To the west, a forebulge persisted as a result of the weight of the glaciers present to the east and north

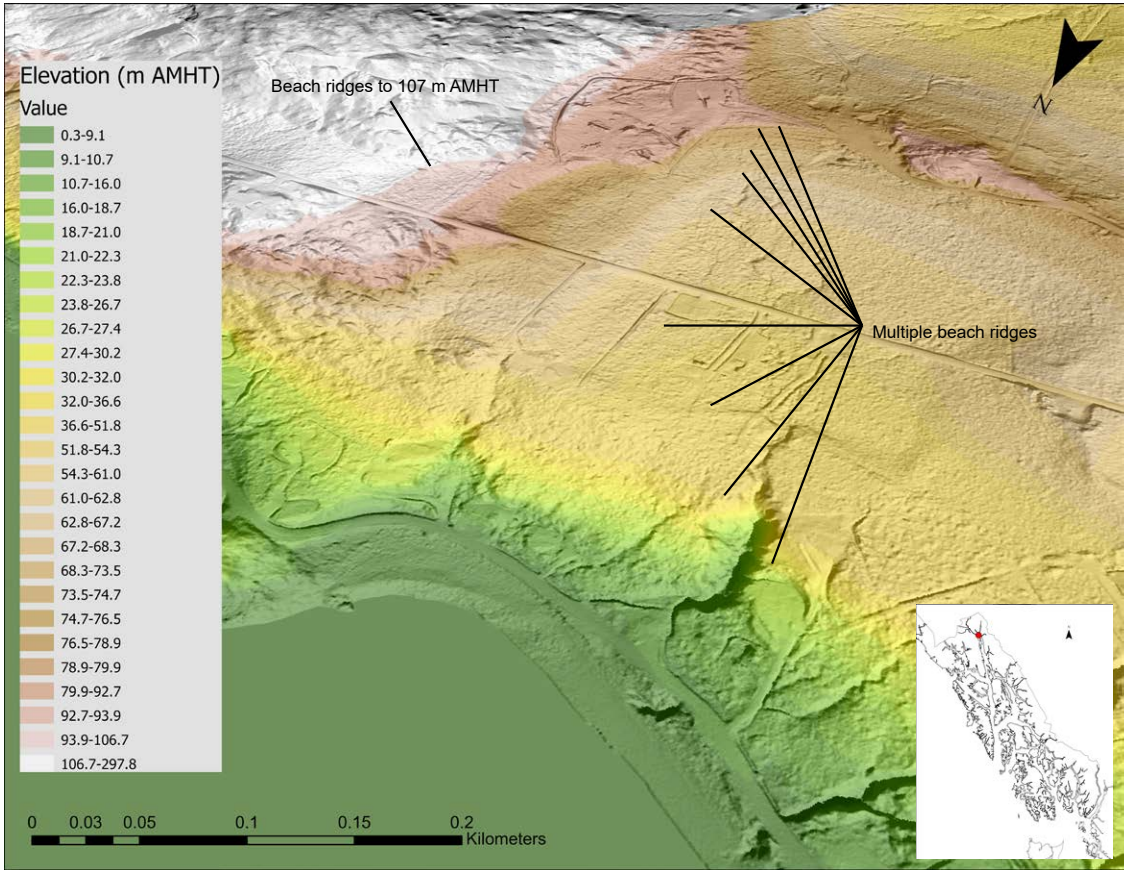

Figure 12. Example of the shorelines interpreted from lidar data acquired in 2014 and 2020 (Alaska Division of Geologic and Geophysical Surveys elevation portal; https://elevation.alaska.gov/) near Haines, Alaska, on the mainland. The center of the image is approximately at 59.224794°N, 135.431657°W. The lidar data show at least 26 storm berms and wave-eroded shorelines up to 107 m above sea level (Alaska Division of Geologic and Geophysical Surveys elevation portal; https://elevation.alaska.gov/). Though undated, shell fragments have been discovered in the 107 m AMHT storm berm (J. P. Norton, 2021, personal commun.) Breaks in the color scheme show the elevation of these berms and shorelines. AMHT—above mean high tide.

and isolated ice caps on islands. This forebulge is expected to have changed in breadth and magnitude as the glaciers receded and thinned. The Queen Charlotte fault became the western terminus of the forebulge (Barrie et al., 2021).

To the east, the land was isostatically depressed by the weight of the ice. As the glaciers receded and sedimentation along the fjord sides and the glacial fronts slowed, marine organisms became established. First, those organisms that could tolerate the dynamics and energy of the changing landscape took hold; later, intertidal and near-tidal communities somewhat similar to those of the modern day became established. By 14,870 ± 630 to 12,820 ± 340 cal. yr B.P., most of the fjords and straits were ice free, and early mollusk communities became established.

As the main body of the CIS retreated toward interior British Columbia at ca. 14,500 cal. yr B.P. (Lesnek et al., 2020), isolated or stranded ice caps likely persisted on many of the islands in southeastern Alaska. Valleys throughout the region were likely occupied by alpine glaciers (Lesnek, et al., 2020). During intervals of high sea level, seaward portions of modern coastal river systems such as the Taku, Stikine, and Unuk Rivers in Alaska and the Iskut and Nass Rivers in British Columbia would have been submerged, providing habitat for marine organisms (Buddington and Chapin, 1929; McConnell, 1913; Twenhofel, 1952). Glaciers occupying these valleys would have rapidly calved back to fjord heads in response to relative sea-level rise (Clague and James, 2002). Furthermore, many of the largest islands such as Admiralty, Kupreanof, Kuiu, and Mitkof would have consisted of several smaller islands at that time.

Though not dated, foraminifera have been documented from a glaciomarine diamicton at an elevation of 211 m on northern Admiralty Island (Miller, 1973a). In the vicinity of Mitkof, Wrangell, and Etolin Islands, shell-bearing strata can be found up to 72 m asl (Yehle, 1978). Near Revillagigedo

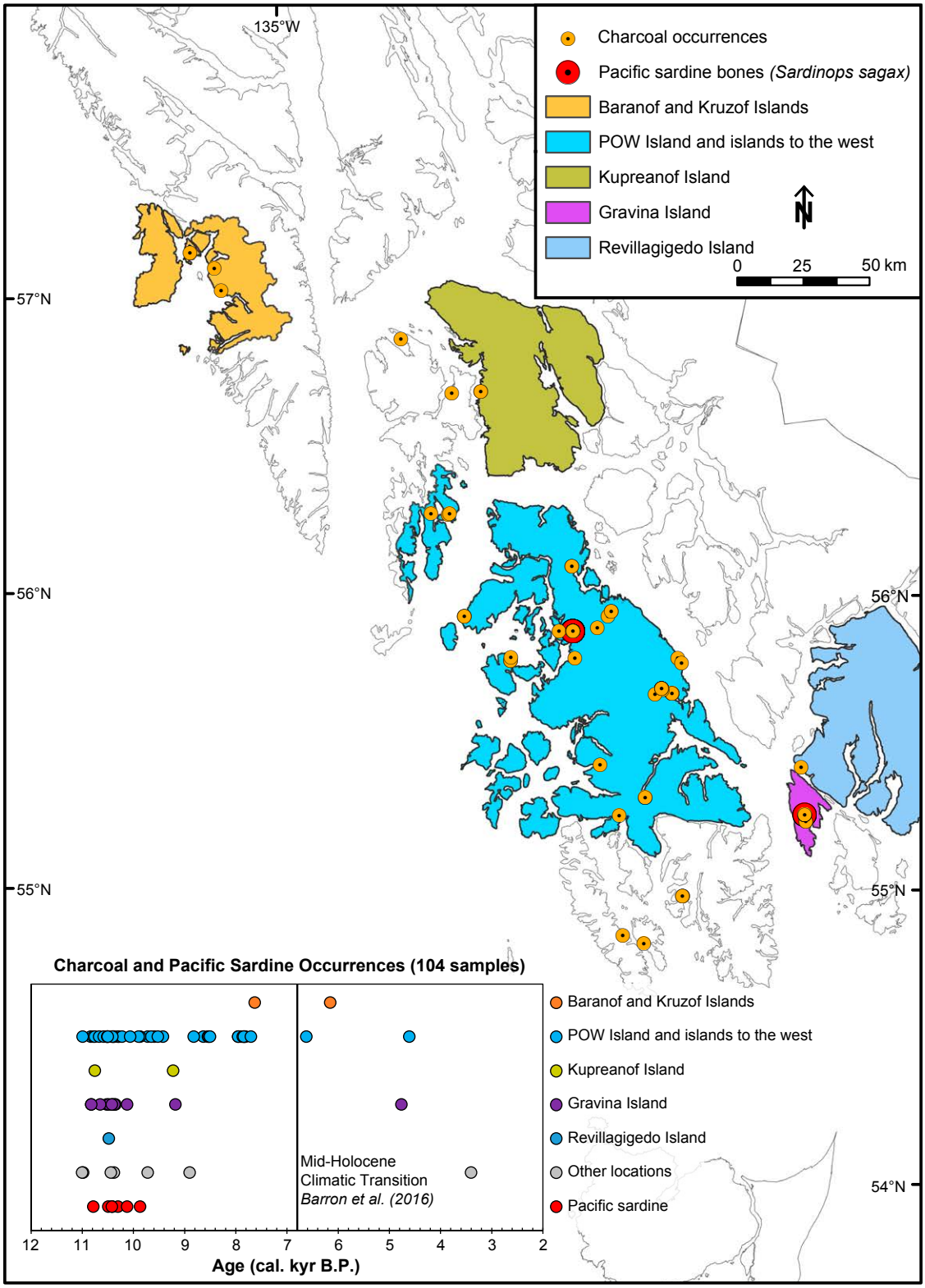

Figure 13. Map showing the locations of the samples that contain charcoal and Pacific sardine (*Sardinops sagax*). This figure includes a graph showing occurrences of charcoal and Pacific sardine from shell-bearing strata across the study area by age and island group. Note that the color symbols and spatial extents of these island groups differ from those presented in Figure 2. POW—Prince of Wales Island; cal.—calibrated.

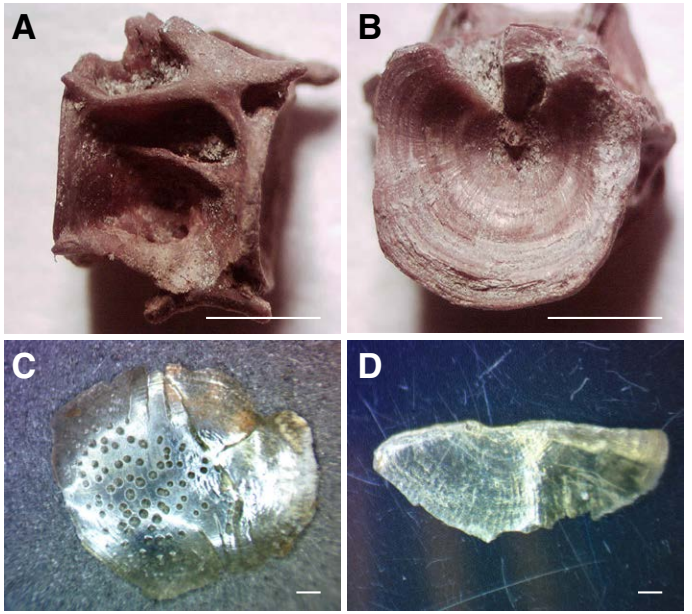

Figure 14. Pacific sardine (*Sardinops sagax*) vertebrae and scales from Yatuk Creek on Prince of Wales Island and Bostwick Creek on Gravina Island. The vertebrae in images A and B were recovered from Yatuk Creek and date to 9870 ± 640 calibrated yr B.P. The scales in images C and D were recovered from Bostwick Creek and date to 10,780 ± 570 cal. yr B.P. White bar is ~1 mm.

Island, shell-bearing strata are found up to 80 m asl. In the vicinity of the Juneau mainland and Douglas and northern Admiralty Islands, shell-bearing strata can be found up to an elevation of 191 m asl (Fig. 3J). These deposits lie ~0.30 m beneath what appears to be the Mount Edgecumbe dacite tephra (Fig. 6). Age constraints on the tephra range from 13,582–12,769 cal. yr B.P. (Riehle et al., 1992a, 1992b; Begét and Motyka, 1998; Dunning, 2011; Baichtal, 2014). The Mount Edgecumbe dacite tephra serves as a marker horizon across much of the central and northern portions of the study area (Riehle et al., 1992b) and has been found in both terrestrial and marine records (Addison et al., 2010; Dunning, 2011). Several tephras lie stratigraphically below the Mount Edgecumbe dacite tephra, some of which have been attributed to other Mount Edgecumbe volcanic field eruptions and the Wrangell volcanic field (Addison et al., 2010; Dunning, 2011). A precise age for these earlier eruptions has not been determined, but Ager (2019) reported the presence of two tephras with ages of 14,600 and 13,760 cal. yr B.P. in a lake on Baranof Island. We identified two sites near Juneau (sample IDs DOUGLAS13, DOUGLAS31, DOUGLAS32, JUNEAU23, and JUNEAU68; Table S1 [see footnote 1]) that appear to contain Mount Edgecumbe dacite tephra similar to that described near Montana Creek by Begét and Motyka (1998).

The variable marine limit between the oldest dated sites from the inner zones of the study area reflects the differential loading of glacial ice and the isostatic response of the landscape. The shell-bearing strata have not been analyzed to determine the likely depth of deposition based on the mollusk and foraminifera species composition. Though at widely varying elevations from current sea level to 191 m asl, as discussed above, the oldest dated sites from the inner zones of the study area that overlap at 2σ range in age from 14,870 ± 630 to 12,820 ± 340 cal. yr B.P. Shortly after ca. 14,000 cal. yr B.P., land surfaces in the Juneau–Douglas Island–northern Admiralty Island region rapidly rose. Most landscapes had rebounded to within 25 to 30 m of present sea level by the beginning of the Younger Dryas at 12,900 cal. yr B.P. (Figs. 3E, 3F, 3G, 3H, 3I, and 3J). This means in the Juneau, Douglas Island, and northern Admiralty Island vicinity the land rose a minimum of 180 m in 2800 yr. In approximately the same amount of time, the land rose 35 m near Mitkof and Wrangell Islands and 50 m near Ketchikan, Alaska.

Collapse of the Crustal Forebulge

West of the CIS margins, a forebulge had developed as the ice retreated. This forebulge is similar in breadth and timing to that described by Hetherington et al. (2003, 2004) and Barrie et al. (2014) along the northern coast of British Columbia. Though undated, a terrace 165 m below sea level (bsl) is visible on multibeam bathymetry throughout southeastern Alaska (Carlson, 2007; Shugar et al., 2014). Terraces at 180 m to 170 m bsl are visible to the west of Kruzof Island (Greene et al., 2007, 2011). These terraces are similar to those described by Barrie and Conway (2012) in Hecate Strait between Haida Gwaii and the British Columbia mainland. We have no core data near these terraces for approximating their age; however, these terraces very likely predate the beginning of the Younger Dryas and mark where the fetch of the sea came into equilibrium with the forebulge front sometime before the glaciers fully retreated from the fjords and straits at ca. 14,000 cal. yr B.P.

Carlson and Baichtal (2015) first reported evidence of a forebulge along the western shore Prince of Wales Island from many of the islands immediately to the west. Baichtal et al. (2017a, 2017b) further discussed and defined the forebulge and associated sea-level fluctuations. Our analysis has refined the timing and description of this forebulge. Additional evidence for the development of a forebulge has been reported from four submerged localities; three sets of cores retrieved off the western coast of southeastern Alaska recorded the sea breaching basin sills in what are now saltwater basins (Barron et al., 2009; Addison et al., 2010; Barrie et al., 2021).

In Sitka Sound, a core (EW0408-40JC) obtained west of Baranof Island and south of Kruzof Island constrains the collapse of the northern edge of

the forebulge off Baranof Island, tracking the shift of Sitka Sound from an isolated lacustrine environment to marine (Addison et al., 2010). The core records the breaching of a sill at 113 m bsl. A radiocarbon-dated bivalve 0.39 m above the breach record provides a minimum-limiting age of the inundation at 11,730–12,670 cal. yr B.P. (median age of 12,200 ± 480 cal. yr B.P.). Given that eustatic sea level was 61 m lower than today at that time (Peltier and Fairbanks, 2006), a 52-m-high forebulge was required to create the basin sill.

In the Gulf of Esquibel, west of Prince of Wales Island and south of Heceta Island, core EW0408-11JC (Barron et al., 2009) records sedimentation in the basin defined by a sill at 80 m bsl. Here, a bivalve provides a minimum age of 12,260–11,350 cal. yr B.P. (median age of 11,805 ± 455 cal. yr B.P.) for the flooding of the gulf, though underlying sediments are rich in sea-ice and freshwater diatoms and/or silicoflagellates mirroring the Younger Dryas freshening event described by Praetorius et al. (2020). Below these sediments lies a tephra correlated to a tephra in Leech Lake and possibly a tephra in a core from the Bald Mountain bog, both on Heceta Island (T.A. Ager, 2021, personal commun.). Wilcox et al. (2019a) dated a correlative black basaltic tephra from a lake on Baker Island to 13,492 ± 237 cal. yr B.P. Given the absence of Bølling-Allerød signatures between the tephra and the apparently Younger Dryas sediments (and the otherwise surprisingly low sedimentation rate linking the two stratigraphic markers), core EW0408-11J likely experienced a similar erosive event by the transgression of the sea early in the Younger Dryas that removed any sedimentation that occurred during the preceding period. Given that eustatic sea level then was 58 m lower than today (Peltier and Fairbanks, 2006), there must have been a 22-m-high forebulge to create the basin sill at that time.

Three cores reported by Barrie et al. (2021) southwest of Suemez Island further illuminate the shifts surrounding the collapse of the outer forebulge and rapid transgression of the sea, an erosive process. Radiocarbon dates on bivalves in marine muds, presumably representing an age prior to exposure (under an erosional boundary), and ages of bivalves bracketing a layer of coarse gravels and sands immediately following the transgression overlap significantly, a function of natural variability in the marine reservoir effect and plateaus in the radiocarbon calibration curve producing multiple intercepts during the Younger Dryas. Despite the lack of precision, these overlapping ages constrain the shifts between a shallow-marine, potentially subaerially exposed, and resubmerged landscape between 12,650 and 12,050 cal. yr B.P. Unfortunately, the cores do not provide linkages between the timing of the forebulge collapse and forebulge elevations. Bathymetry for the area is incomplete, so at this time we cannot determine whether the core locations are representative of the forebulge or lie in isolated basins. Core 201504-41 from 138.5 m bsl provides an appropriate elevation minimum, producing a dated bivalve providing a minimum age for the collapse of the forebulge between 12,410 and 11,580 cal. yr B.P., with a median age of 11,995 ± 415 cal. yr B.P. The sea level at that time was 59 m bsl. For this basin to have flooded, a forebulge of 80 m must have existed.

As the forebulge migrated eastward and collapsed, it marked the uppermost elevation of the maximum sea-level transgression, which can be seen on lidar data acquired in 2017 and 2018. Glacial features and fluvial terraces are clearly truncated at 19 m to 25 m above AMHT (Fig. 8). The highest shorelines are found on northeastern and southern Prince of Wales Island at 25 m AMHT. Glacially carved troughs, submarine moraines, and ice-flow indicators such as striations and drumlins suggest that the thick ice streams occupying Sumner Strait to the north and Dixon Entrance to the south flowed over Prince of Wales Island (Lesnek et al., 2020). Thus, we attribute the differences in maximum shoreline elevation across this zone to variable CIS loading during the Late Pleistocene. Six distinct terraces can be seen below the erosion of the glacial and fluvial features. Carlson and Baichtal (2015) attempted to define the timing and extent of these terraces to the location of early Holocene archaeological sites using the occurrences of shell-bearing strata; >30 sites have been found using this methodology (Carlson, 2017; Schmuck, 2021). However, the oldest shell deposits predate the oldest known cultural deposits by ~40–700 yr. We interpret the age of these oldest deposits as a minimum-limiting age for the transgression associated with the collapse of the forebulge. Seventeen (17) of the oldest dated deposits within 2σ uncertainty range from southwestern Kuiu, Kosciusko, Heceta, and western Prince of Wales Islands date to 11,000 ± 390 to 10,500 ± 420 cal. yr B.P. (Fig. 7). We suggest this range is a minimum-limiting age for the collapse of the forebulge. Once the forebulge had collapsed and the shoreline had reached equilibrium, intertidal communities rapidly developed. Therefore, these older shell deposits do not provide the precise timing of the end of the forebulge collapse, but date to a time shortly after when intertidal communities became re-established. During this interval, the land was rising due to ongoing isostatic and tectonic adjustments, and within 40–700 yr, the wave-eroded terraces and deltas began to re-emerge. The six distinct terraces identified on lidar imagery suggest periods where eustatic sea level and isostatic uplift came into equilibrium long enough to result in either (1) erosion of a terrace at the maximum height of the sea or (2) deposition of a delta at the mouth of a fluvial system delivering sediment to the ocean.

Near Sitka on Baranof Island, the uppermost elevation of the maximum sea-level transgression as the forebulge to the west collapsed is much lower in elevation than on western Prince of Wales Island. The highest, oldest shell bed dates to 7930 ± 390 cal. yr B.P. at an elevation of 4.0 m AMLLW on Krestof Island to the west of Baranof Island (Fig. 5C). The explosive dacite eruption of Mount Edgecumbe on Kruzof Island blanketed the Sitka vicinity with tephra as much as 1 m deep at ca. 13,165 ± 85 cal. yr B.P. (Riehle et al., 1992a, 1992b; Begét and Motyka, 1998; Baichtal, 2014). The upper limit of the maximum transgression in the Sitka region is marked by the contact between the Mount Edgecumbe tephra and underlying bedrock. At elevations of up to 9.0 m AMLLW, the tephra has been eroded by wave action, exposing Quaternary basalt flows (Riehle et al., 1992a, 1992b) and Sitka Graywacke (Karl et al., 2015). In a few outcrops and where power-pole holes have been drilled, a storm berm consisting of wave-rounded cobbles running

parallel to the paleoshoreline has been exposed. Some 5 m below the highest storm berm deposit is the upper limit of the shell-bearing strata (Fig. 5D).

Southeastern Alaska Paleoenvironments Inferred from Charcoal and Pacific Sardine Occurrences

Charcoal is particularly abundant in samples dating from 11,000 ± 390 to 7630 ± 90 cal. yr B.P. during what is inferred to be the local Holocene Climatic Optimum (Fig. 13). This interpretation is supported by the presence of Pacific sardine (*Sardinops sagax*) bones in charcoal deposits ranging in age from 10,780 ± 570 to 9870 ± 640 cal. yr B.P. (Figs. 13 and 14). In modern times, the habitat range of this fish species does not typically extend to southeastern Alaska; however, Pacific sardine has been observed in the region following the exceptionally warm, strong El Niño events in 1930–1931 and 1997–1998 (Wing et al., 2000). In the broader northeastern Pacific region, northward expansions of Pacific sardine habitats were also documented during the 2013–2015 El Niño event (Cavole et al., 2016). Anomalously warm El Niño events involve increased temperatures in the North Pacific, which may explain the change in habitat range of Pacific sardine observed during these intervals (Wing et al., 2000). Therefore, occurrences of Pacific sardine between ca. 10,800 and ca. 9900 cal. yr B.P. in southeastern Alaskan sediments suggest the presence of strong El Niño events and/or a warmer regional climate during the early Holocene (Carlson, 2007).

Biological proxies in terrestrial and marine sediment cores also suggest a warm early Holocene in southeastern Alaska. Heusser et al. (1985) reported on data derived from fossil pollen contained in two sections of muskeg located near Munday Creek on the Gulf of Alaska, ~15 km northwest of Icy Cape in the Malaspina Glacier district; one section extends to ca. 10,200 cal. yr B.P., whereas the other reaches to beyond ca. 12,800 cal. yr B.P. They reported mean July temperatures of ~14 °C at the end of the Pleistocene (11,700 cal. yr B.P.) and in the early Holocene, reaching a maximum ~16 °C at ca. 8900 cal. yr B.P., then decreasing to 12 °C by ca. 6000 cal. yr B.P. Annual precipitation, just under 1400 mm at the beginning of the record, reached a minimum ~1200 mm coinciding with the temperature maximum at 8900 cal. yr B.P. Ager (2019) also described an early Holocene warming with a mid-Holocene temperature shift to cooler, wetter conditions. These findings correlate closely to the time period in which we find the most abundant charcoal in the shell-bearing sediments. Barron et al. (2016) described diatom and silicoflagellate assemblages documented in cores EW0408-47JC, EW0408-47MC, and EW0408-46MC from the outer portion of Slocum Arm from western Chichagof Island. The base of the core (sample depth 1.78 m below seafloor) dates to 10,176–9746 cal. yr B.P. (Barron et al., 2016). They suggested that the record from the early portion of the core (>ca. 6800 cal. yr B.P.) contains oceanic diatoms indicative of cold winters and warm summers. Praetorius et al. (2015) documented a 4–5 °C warming event in the Gulf of Alaska during the transition into the early Holocene (11,400–10,900 cal. yr B.P.). This interval corresponds with the timing of the most abundant charcoal and the presence of Pacific sardine from our samples.

The coincidence of abundant charcoal in southeastern Alaskan raised shell-bearing marine deposits with warmer climate in the early Holocene and rarity of charcoal in the cooler middle and late Holocene raised marine deposits suggest a linkage between forest-fire history and climate in southeastern Alaska, as reported in neighboring British Columbia (Brown and Hebda, 2002, 2003). It is tempting to speculate on a potential anthropogenic source for charcoal in southeastern Alaska marine deposits predating confirmed archaeological evidence for humans. In coastal British Columbia, evidence for late Holocene anthropogenic forest fires has been used to argue for charcoal as a possible proxy for human presence in the absence of archaeological evidence (Hoffman et al., 2017; Mathewes et al., 2019). Archaeological evidence suggests a constant human presence since ca. 10,500 cal. yr B.P. in southeastern Alaska (Carlson 2007, 2012; Carlson and Baichtal, 2015). If the charcoal in the raised shell-bearing strata was cultural in origin, one would expect it to be present throughout all of the Holocene. Charcoal is conspicuously absent in the late Holocene sediments (≥7630 ± 90 cal. yr B.P.). In southeastern Alaska, the charcoal occurring in the raised marine sediments is not likely to be anthropogenic and instead records periods of increased naturally triggered forest-fire activity.

Establishment of Early Inhabitants and Environmental Hazards

If humans were present in southeastern Alaska in the immediate postglacial period, what environmental hazards may they have faced? Following retreat of the CIS, intertidal mollusk species traditionally used for food began to reappear across the Northwest Coast by around 14,200 cal. yr B.P. (Schmuck et al., 2021). However, the establishment of the willow-sedge and pine parklands on land (Ager, 2019) was tempered by intense volcanism; the Mount Edgecumbe volcanic field alone was responsible for 22 individual eruptions in central southeastern Alaska, 19 within a peak interval between 14,600 and 13,100 cal. yr B.P. (Praetorius et al., 2016). There is mounting evidence for further eruptions from other volcanic fields in the southern part of southeastern Alaska at the end of that interval (Wilcox et al., 2019a; T.A. Ager, 2021, personal commun.). Furthermore, if coastal fisher-gatherers lived along the outer coast of southeastern Alaska by this time, rapid sea-level rise accompanying the collapse of the forebulge would likely have been recognizable at a human scale (Mackie et al., 2014). In all, these factors would have contributed to a dynamic environment for human occupation during the Late Pleistocene.

SUGGESTIONS FOR FUTURE WORK

We hope that this data set and discussion will be a catalyst for further research into the late Quaternary history of the study area. Here, we offer a few suggestions for further study. A logical next step is to integrate the chronology presented here with the elevations of beach ridges apparent on lidar

bare-earth models in a geophysical model. This exercise would result in a range of plausible relative sea-level curves for southeastern Alaska that can be directly compared to those presented here to assess crustal response to ice loading, constrain the possible range of ice thicknesses, or gain a better understanding of the region's mantle rheology. Faunal analysis of shell-bearing sediments holds a wealth of potential for determining the probable depth of deposition, salinity, and water temperature of these deposits, which could help to further refine the relative sea-level curves presented here and add information about environmental conditions through time. Fully dating and characterizing the now-submerged pāhoehoe lava flows and eruptive centers off the western coast of southeastern Alaska is necessary for linking these geomorphic features with tephra observed in sediment cores across the region, which has implications for both the region's glacial history and volcanic hazard assessments. Future marine sediment cores targeting closed basins at different elevations to determine the rate of sea-level rise is paramount in defining the timing and persistence of the forebulge along the western margin of the study area. Coupled with the sampling of marine basins, targeted sampling of Younger-Dryas and Bølling-Allerød marine deposits for shell-wood pairs is necessary for further refining the marine-reservoir-effect calibrations used to date shellfish, our proxies for sea-level change, in these critical periods. At present, the calibration curve used here is a regional synthesis of pairs from across the Northwest Coast (Schmuck et al., 2021). Further sample pairs from southeastern Alaska would provide a means to account for regional variation driven by the "hard water effect" of karst groundwaters.

The intense erosional processes described by Barrie et al. (2021) leave little hope for Late Pleistocene archaeological site survival on the once-exposed western coastal plain or in potential refugia on the now-submerged outer forebulge. Unlike on the eastern edge of Haida Gwaii, where shallow bays and a broad coastal plain are sheltered from wave action (Mackie et al., 2014), the waterways of the Alexander Archipelago are deeply incised channels that offer scant protection for submerged sites. Nevertheless, exploratory surveys guided by relative sea-level reconstructions (e.g., Carlson and Baichtal, 2015; McLaren et al., 2014, 2018, 2020) have demonstrated great promise in locating ancient cultural sites on the Pacific coast. Targeting similar areas above modern sea level in southeastern Alaska, particularly those near "sea-level hinges" (McLaren et al., 2014) where relative sea level has not changed significantly since deglaciation, may reveal pre-Holocene archaeological sites.

Southeastern Alaska is the ancestral homeland of the Tlingit, who remember the complex relationship between their people and sea-level change in oral traditions (Worl, 2010). If this communal memory records human-environment interaction in the region as far back as the Younger Dryas or Bølling-Allerød, it suggests that older cultural sites in danger of disturbance by modern development may exist in areas that have not yet been recognized by archaeologists. Many of the early Holocene sites first identified in southeastern Alaska were discovered during the destructive building of roads and other infrastructure (Carlson and Baichtal, 2015). Articulating the timing and prior extents of relative sea-level change across the landscape are critical for identifying and protecting ancient cultural sites in the future. Finally, two-way exchange with scientific results like these being communicated back to the native communities should be common to all future work.

ACKNOWLEDGMENTS

The Tongass National Forest Geology Program has supported and funded this research for 30 years, as has the University of Alaska Southeast, Juneau. Many people through the years have contributed to discovery and sampling of shell-bearing strata throughout southeastern Alaska, many more than can be named here. Cathy Connor, Greg Streveler, Daniel Monteith, Rachel Myron, Jacqueline de Montigny, John Norton, Terry Brock, Linda Slaght, Gina Esposito, Gene Primaky, Kris Larson, David Love, and Katherine Prussian have supported data collection over the years. Susan Karl with the U.S. Geological Survey in Anchorage has been instrumental in both data collecting and interpretation, providing invaluable assistance. A special thanks to Susan Crockford of Pacific Identifications Inc., Victoria, British Columbia, for fish species identification. We would like to thank James Vaughn Barrie, Geological Survey of Canada, and Daniel Shugar, Department of Geoscience, University of Calgary, for their reviews and thoughtful comments that improved this manuscript.

REFERENCES CITED

Addison, J.A., Beget, J.E., Ager, T.A., and Finney, B.P., 2010, Marine tephrochronology of the Mt. Edgecumbe Volcanic Field, Southeast Alaska, USA: Quaternary Research, v. 73, p. 277–292, https://doi.org/10.1016/j.yqres.2009.10.007.

Ager, T.A., 2019, Late Quaternary vegetation development following deglaciation of northwestern Alexander Archipelago, Alaska: Frontiers of Earth Science, v. 7, 104, https://doi.org/10.3389/feart.2019.00104.

Baichtal, J.F., 2014, The buried forest of Alaska's Kruzof Island: A window into the past: U.S. Department of Agriculture Blog Archives, https://www.usda.gov/media/blog/2014/03/07/buried-forest-alaskas-kruzof-island-window-past (accessed March 2021).

Baichtal, J.F., and Carlson, R.J., 2010, Development of a model to predict the location of early Holocene habitation sites along the western coast of Prince of Wales Island and the outer islands, Southeast Alaska: Current Research in the Pleistocene, v. 27, p. 64–66.

Baichtal, J.F., Carlson, R.J., Smith, J.L., and Landwehr, D.J., 2017a, Defining the timing and extent of the marine transgression following the Last Glacial Maximum in southeastern Alaska: Geological Society of America Abstracts with Programs, v. 49, no. 6, https://doi.org/10.1130/abs/2017AM-298879.

Baichtal, J.F., Carlson, R.J., Smith, J.L., and Landwehr, D.J., 2017b, Reconstructing southeast Alaska's relative sea level history from raised shell-bearing strata and narrowing the timing of the retreat of the Cordilleran ice sheet from the archipelago to near 13.700 Cal. BP, *in* Program with Abstracts, 47th Annual International Arctic Workshop, March 23–25, 2017, Buffalo, New York, p. 33–36.

Barclay, D.J., Calkin, P.E., and Wiles, G.C., 2001, Holocene history of Hubbard Glacier in Yakutat Bay and Russell Fjord, southern Alaska: Geological Society of America Bulletin, v. 113, p. 388–402, https://doi.org/10.1130/0016-7606(2001)113<0388:HHOHGI>2.0.CO;2.

Barrie, J.V., and Conway, K.W., 2002, Rapid sea-level change and coastal evolution on the Pacific margin of Canada: Sedimentary Geology, v. 150, p. 171–183, https://doi.org/10.1016/S0037-0738(01)00274-3.

Barrie, J.V., and Conway, K.W., 2012, Paleogeographic reconstruction of Hecate Strait, British Columbia: Changing sea levels and sedimentary processes reshape a glaciated shelf, *in* Li, M.Z., Sherwood, C.R., and Hill, P.R., eds., Sediments, Morphology and Sedimentary Processes on Continental Shelves: Advances in Technologies, Research, and Applications: International Association of Sedimentologists Special Publication 44, p. 29–46, https://doi.org/10.1002/9781118311172.ch2.

Barrie, J.V., Hetherington, R., and Macleod, R., 2014, Pacific margin, Canada shelf physiography: A complex history of glaciation, tectonism, oceanography and sea-level change, *in* Chiocci, F.L., and Chivas, A.R., eds., Continental Shelves of the World: Their Evolution During the Last Glacio-Eustatic Cycle: Geological Society of London Memoir 41, p. 305–313, https://doi.org/10.1144/M41.22.

Barrie, J.V., Greene, H.G., Conway, K.W., and Brothers, D.S., 2021, Late Quaternary sea level, isostatic response, and sediment dispersal along the Queen Charlotte fault: Geosphere, v. 17, p. 375–388, https://doi.org/10.1130/GES02311.1.

Barron, J.A., Bukry, D., Dean, W.E., Addison, J.A., and Finney, B., 2009, Paleoceanography of the Gulf of Alaska during

the past 15,000 years: Results from diatoms, silicoflagellates, and geochemistry: Marine Micropaleontology, v. 72, p. 176–195, https://doi.org/10.1016/j.marmicro.2009.04.006.
Barron, J.A., Bukry, D., Addison, J.A., and Ager, T.A., 2016, Holocene evolution of diatom and silicoflagellate paleoceanography in Slocum Arm, a fjord in southeastern Alaska: Marine Micropaleontology, v. 126, p. 1–18, https://doi.org/10.1016/j.marmicro.2016.05.002.
Begét, J.E., and Motyka, R.J., 1998, New dates on late Pleistocene dacitic tephra from the Mount Edgecumbe volcanic field, southeastern Alaska: Quaternary Research, v. 49, p. 123–125, https://doi.org/10.1006/qres.1997.1945.
Berg, H.C., 1973, Geology of Gravina Island, Alaska: A description of the stratigraphy, lithology, general geology, and mineral resources of a structurally complex 100-square-mile island near Ketchikan, Alaska: U.S. Geological Survey Bulletin 1373, 41 p., https://doi.org/10.3133/b1373.
Braje, T.J., Erlandson, J.M., Rick, T.C., Davis, L., Dillehay, T., Fedje, D.W., Froese, D., Gusick, A., Mackie, Q., McLaren, D., Pitblado, B., Raff, J., Reeder-Myers, L., and Waters, M.R., 2020, Fladmark + 40: What have we learned about a potential Pacific Coast peopling of the Americas?: American Antiquity, v. 85, p. 1–21, https://doi.org/10.1017/aaq.2019.80.
Bronk Ramsey, C., 2009, Bayesian analysis of radiocarbon dates: Radiocarbon, v. 51, p. 337–360, https://doi.org/10.1017/S0033822200033865.
Brown, K.J., and Hebda, R.J., 2002, Origin, development, and dynamics of coastal temperate conifer rainforests of southern Vancouver Island, Canada: Canadian Journal of Forest Research, v. 32, p. 353–372, https://doi.org/10.1139/x01-197.
Brown, K.J., and Hebda, R.J., 2003, Coastal rainforest connections disclosed through a Late Quaternary vegetation, climate, and fire history investigation from the Mountain Hemlock Zone on southern Vancouver Island, British Columbia, Canada: Review of Palaeobotany and Palynology, v. 123, p. 247–269, https://doi.org/10.1016/S0034-6667(02)00195-1.
Buddington, A.F., and Chapin, T., 1929, Geology and mineral deposits of southeastern Alaska: U.S. Geological Survey Bulletin 800, 398 p., https://doi.org/10.3133/b800.
Campbell, C.R., 1995, An archaeological survey of Big Salt Lake Road, Alaska Forest Highway 9, Prince of Wales Island, southeast Alaska: Western Federal Lands Highway Division, Federal Highway Administration, U.S. Department of Transportation Report, Contract DTFH70-94-Q-06, 18 p.
Carlson, R.J., 1984, Analysis of marine shells from Yatuk Creek Rockshelter and unnamed lake marine beach, Prince of Wales Island, southeastern Alaska: Report submitted under contract 53-0109-3-00152 to U.S. Department of Agriculture Forest Service, Alaska Region, Ketchikan, 14 p.
Carlson, R.J., 1991, Field notes on file, United States Forest Service, Craig Ranger District, Craig, Alaska: U.S. Department of Agriculture Report 1991-05-35.
Carlson, R.J., 1992, Raised marine beach inventory, southeast Alaska: U.S. Forest Service,Tongass National Forest, Ketchikan Area, archaeological files.
Carlson, R.J., 2007, Current models for the human colonization of the Americas: The evidence from southeast Alaska [M.Phil. thesis]: Cambridge, UK, University of Cambridge, 67 p.
Carlson, R.J., 2012, A predictive model for early Holocene archaeological sites in Southeast Alaska based on elevated palaeobeaches [Ph.D. thesis]: Cambridge, UK, University of Cambridge, 313 p.
Carlson, R.J., 2017, Raised marine predictive model advances knowledge of early Holocene site assemblages in southern Southeast Alaska, *in* Proceedings, Society for American Archaeology 82nd Annual Meeting, Vancouver, British Columbia, 29 March–2 April, Abstracts, v. 1, p. 134.
Carlson, R.J., and Baichtal, J.F., 2015, A predictive model for locating early Holocene archaeological sites based on raised shell-bearing strata in Southeast Alaska, US: Geoarchaeology, v. 30, p. 120–138, https://doi.org/10.1002/gea.21501.
Cavole, L.M., Demko, A.M., Diner, R.E., Giddings, A., Koester, I., Pagniello, C.M.L.S., Paulsen, M.-L., Ramirez-Valdez, A., Schwenck, S.M., Yen, N.K., Zill, M.E., and Franks, P.J.S., 2016, Biological impacts of the 2013–2015 warm-water anomaly in the northeast Pacific: Winners, losers, and the future: Oceanography (Washington, D.C.), v. 29, no. 2, p. 273–285, https://doi.org/10.5670/oceanog.2016.32.
Clague, J.J., 1983, Glacio-isostatic effects of the Cordilleran ice sheet, British Columbia, Canada, *in* Smith, D.E., and Dawson, A.G., eds., Shorelines and Isostasy: Institute of British Geographers Special Publication 16, p. 321–343.
Clague, J.J., and James, T.S., 2002, History and isostatic effects of the last ice sheet in southern British Columbia: Quaternary Science Reviews, v. 21, p. 71–87, https://doi.org/10.1016/S0277-3791(01)00070-1.
Clague, J., Harper, J.R., Hebda, R.J., and Howes, D.E., 1982a, Late Quaternary sea levels and crustal movements, coastal British Columbia: Canadian Journal of Earth Sciences, v, 19, p. 597–618, https://doi.org/10.1139/e82-048.
Clague, J.J., Mathewes, R.W., and Warner, B.G., 1982b, Late Quaternary geology of eastern Graham Island, Queen Charlotte Islands, British Columbia: Canadian Journal of Earth Sciences, v. 19, p. 1786–1795, https://doi.org/10.1139/e82-157.
Clark, P.U., Dyke, A.S., Shakun, J.D., Carlson, A.E., Clark, J., Wohlfarth, B., Mitrovica, J.X., Hostetler, S.W., and McCabe, A.M., 2009, The Last Glacial Maximum: Science, v. 325, p. 710–714, https://doi.org/10.1126/science.1172873.
Connor, C., Streveler, G., Post, A., Monteith, D., and Howell, W., 2009, The Neoglacial landscape and human history of Glacier Bay, Glacier Bay National Park and Preserve, southeast Alaska, USA: The Holocene, v. 19, p. 381–393, https://doi.org/10.1177/0959683608101389.
Daanen, R.P., Herbst, A.M., Wikstrom Jones, K., and Wolken, G.J., 2021, High-resolution lidar data for Haines, Southcentral Alaska, December 8–12, 2020: Alaska Division of Geological and Geophysical Surveys Raw Data File 2021-4, 8 p., https://doi.org/10.14509/30595.
Dall, W.M., 1904, Pleistocene fossils from Douglas Island, *in* Merriam, C.H., Emerson, B.K., eds., Washington Academy of Sciences, Harriman Alaska Expedition–1899: Alaska, Volume IV: Geology and Paleontology, by Emerson, B.K., Palache, C., Dall, W.H., Ulrich, E.O., and Knowlton, F.H.: New York, Doubleday, Page & Co., p. 120–122.
Darvill, C.M., Menounos, B., Goehring, B.M., Lian, O.B., and Caffee, M.W., 2018, Retreat of the western Cordilleran Ice Sheet margin during the last deglaciation: Geophysical Research Letters, v. 45, p. 9710–9720, https://doi.org/10.1029/2018GL079419.
Davis, S.D., 1990, Prehistory of southeastern Alaska, *in* Suttles, W., ed., Handbook of North American Indians, Volume 7: Northwest Coast: Washington, D.C., Smithsonian Institution, p. 197–202.
Davis, S.D., Swanson-Iwamoto, K., Lively, R.A., and Bair, G.A., 1991, Survey design for the cultural resource inventory for the '91 Kelp Bay timber sale, Baranof Island, Alaska: Report for the U.S. Department of Agriculture Forest Service, Tongass National Forest, Sitka, Alaska.
Dunning, H.A., 2011. Extending the applications of tephrochronology in northwestern North America [M.S. thesis]: Edmonton, University of Alberta, 187 p.
Dyke, A.S., 2004, An outline of North American deglaciation with emphasis on central and northern Canada, *in* Ehlers, J., and Gibbard, P.L., eds., Quaternary Glaciations—Extent and Chronology, Part II: North America: Amsterdam, Elsevier, Developments in Quaternary Sciences, v. 2, Part B, p. 373–424, https://doi.org/10.1016/S1571-0866(04)80209-4.
Fedje, D.W., and Christensen, T., 1999, Modeling paleoshorelines and locating early Holocene coastal sites in Haida Gwaii: American Antiquity, v. 64, p. 635–652, https://doi.org/10.2307/2694209.
Fedje, D.W., and Josenhans, H., 2000, Drowned forests and archaeology on the continental shelf of British Columbia, Canada: Geology, v. 28, p. 99–102, https://doi.org/10.1130/0091-7613(2000)28<99:DFAAOT>2.0.CO;2.
Fedje, D., McLaren, D., James, T.S., Mackie, Q., Smith, N.F., Southon, J.R., and Mackie, A.P., 2018, A revised sea level history for the northern Strait of Georgia, British Columbia, Canada: Quaternary Science Reviews, v. 192, p. 300–316, https://doi.org/10.1016/j.quascirev.2018.05.018.
Gaglioti, B.V., Mann, D.H., Wiles, G.C., Jones, B.M., Charlton, J., Wiesenberg, N., and Andreu-Hayles, L., 2019, Timing and potential causes of 19th-century glacier advances in coastal Alaska based on tree-ring dating and historical accounts: Frontiers of Earth Science, v. 7, 82, https://doi.org/10.3389/feart.2019.00082.
Greene, H.G., O'Connell, V.M., Wakefield, W.W., and Brylinsky, C.K., 2007, The offshore Edgecumbe lava field, southeast Alaska: Geologic and habitat characterization of a commercial fishing ground, *in* Todd, B.J., and Green, H.G., eds., Mapping the Seafloor for Habitat Characterization: Geologic Association of Canada Special Paper 47, p. 277–296.
Greene, H.G., O'Connell, V.M., and Brylinsky, C.K., 2011, Tectonic and glacial related seafloor geomorphology as possible demersal shelf rockfish habitat surrogates—Examples along the Alaskan convergent transform plate boundary: Continental Shelf Research, v. 31, no. 2, p. S39–S53, https://doi.org/10.1016/j.csr.2010.11.004.
Hastings, K., 2005, Long-term persistence of isolated fish populations in the Alexander Archipelago [Ph.D. thesis]: Missoula, University of Montana, 210 p., https://scholarworks.umt.edu/etd/9560.
Heaton, T.J., Köhler, P., Butzin, M., Bard, E., Reimer, R.W., Austin, W.E.N., Bronk Ramsey, C., Grootes, P.M., Hughen, K.A., Kromer, B., Reimer, P.J., Adkins, J., Burke, A., Cook, M.S., Olsen, J., and Skinner, L.C., 2020, Marine20—The marine radiocarbon age calibration curve (0–55,000 cal BP): Radiocarbon, v. 62, p. 779–820, https://doi.org/10.1017/RDC.2020.68.
Hetherington, R., and Barrie, J.V., 2004, Interaction between local tectonics and glacial unloading on the Pacific margin of Canada: Quaternary International, v. 120, p. 65–77, https://doi.org/10.1016/j.quaint.2004.01.007.

Hetherington, R., Barrie, J.V., Reid, R.G.B., MacLeod, R., Smith, D.J., James, T.S., and Kung, R., 2003, Late Pleistocene coastal paleogeography of the Queen Charlotte Islands, British Columbia, Canada, and its implications for terrestrial biogeography and early postglacial human occupation: Canadian Journal of Earth Sciences, v. 40, p. 1755–1766, https://doi.org/10.1139/e03-071.

Hetherington, R., Barrie, J.V., Reid, R.G.B., MacLeod, R., and Smith, D.J., 2004, Paleogeography, glacially-induced displacement, and late Quaternary coastlines on the continental shelf of British Columbia, Canada: Quaternary Science Reviews, v. 23, p. 295–318, https://doi.org/10.1016/j.quascirev.2003.04.001.

Heusser, C.J., Heusser, L.E., and Peteet, D.M., 1985, Late-Quaternary climatic change on the American North Pacific Coast: Nature, v. 315, p. 485–487, https://doi.org/10.1038/315485a0.

Hoffman, K.M., Lertzman, K.P., and Starzomski, B.M., 2017, Ecological legacies of anthropogenic burning in a British Columbia coastal temperate rainforest: Journal of Biogeography, v. 44, p. 2903–2915, https://doi.org/10.1111/jbi.13096.

James, T.S., Hutchinson, I., and Clague, J.J., 2002, Improved relative sea-level histories for Victoria and Vancouver, British Columbia: Geological Survey of Canada Current Research 2002-A16, 7 p., https://doi.org/10.4095/213083.

Josenhans, H.W., Fedje, D.W., Conway, K.W. and Barrie, J.V., 1995, Post glacial sea levels on the Western Canadian continental shelf: Evidence for rapid change, extensive subaerial exposure, and early human habitation: Marine Geology, v. 125, p. 73–94, https://doi.org/10.1016/0025-3227(95)00024-S.

Josenhans, H., Fedje, D., Pienitz, R., and Southon, J., 1997, Early humans and rapidly changing Holocene sea levels in the Queen Charlotte Islands–Hecate Strait, British Columbia, Canada: Science, v. 277, p. 71–74, https://doi.org/10.1126/science.277.5322.71.

Karl, S.M., Haeussler, P.J., Himmelberg, G.R., Zumsteg, C.L., Layer, P.W., Friedman, R.M., Roeske, S.M., and Snee, L.W., 2015, Geologic map of Baranof Island, southeastern Alaska: U.S. Geological Survey Scientific Investigations Map 3335, scale 1: 200,000, 82 p. text, https://doi.org/10.3133/sim3335.

Knopf, A., 1912, The Eagle River region, southeastern Alaska: U.S. Geological Survey Bulletin 502, 61 p., 3 sheets, https://doi.org/10.3133/b502.

Lambeck, K., Rouby, H., Purcell, A., Sun, Y., and Sambridge, M., 2014, Sea level and global ice volumes from the Last Glacial Maximum to the Holocene: Proceedings of the National Academy of Sciences of the United States of America, v. 111, p. 15,296–15,303, https://doi.org/10.1073/pnas.1411762111.

Larsen, C.F., Motyka, R.J., Freymueller, J.T., Echelmeyer, K.A., and Ivins, E.R., 2004, Rapid uplift of southern Alaska caused by recent ice loss: Geophysical Journal International, v. 158, p. 1118–1133, https://doi.org/10.1111/j.1365-246X.2004.02356.x.

Larsen, C.F., Motyka, R.J., Freymueller, J.T., Echelmeyer, K.A. and Ivins, E.R., 2005, Rapid viscoelastic uplift in southeast Alaska caused by post–Little Ice Age glacial retreat: Earth and Planetary Science Letters, v. 237, p. 548–560, https://doi.org/10.1016/j.epsl.2005.06.032.

Larsen, C.F., Motyka, R.J., Arendt, A.A., Echelmeyer, K.A., and Geissler, P.E., 2007, Glacier changes in southeast Alaska and northwest British Columbia and contribution to sea level rise: Journal of Geophysical Research, v. 112, F01007, https://doi.org/10.1029/2006JF000586.

Lemke, R.W., 1974, Reconnaissance engineering geology of the Wrangell area, Alaska, with emphasis on evaluation of earthquake and other geologic hazards: U.S. Geological Survey Open-File Report 74-1062, 103 p., 1 sheet, scale 1:7200, https://doi.org/10.3133/ofr741062.

Lemke, R.W., 1975, Reconnaissance engineering geology of the Ketchikan area, Alaska, with emphasis on evaluation of earthquake and other geologic hazards: U.S. Geological Survey Open-File Report 75-250, 65 p., 1 sheet, scale 1:63,360, https://doi.org/10.3133/ofr75250.

Lemke, R.W., and Yehle, L.A., 1972a, Reconnaissance engineering geology of the Haines area, Alaska, with emphasis on evaluation of earthquake and other geologic hazards: U.S. Geological Survey Open-File Report 72-229, 109 p., 2 sheets, scale 1:24,000, https://doi.org/10.3133/ofr72229.

Lemke, R.W., and Yehle, L.A., 1972b, Regional and other general factors bearing on evaluation of earthquake and other geologic hazards to coastal communities of southeastern Alaska: U.S. Geological Survey Open-File Report 72-230, 99 p., https://doi.org/10.3133/ofr72230.

Lesnek, A.J., Briner, J.P., Lindqvist, C., Baichtal, J.F., and Heaton, T.H., 2018, Deglaciation of the Pacific coastal corridor directly preceded the human colonization of the Americas: Science Advances, v. 4, eaar5040, https://doi.org/10.1126/sciadv.aar5040.

Lesnek, A.J., Briner, J.P., Baichtal, J.F., and Lyles, A.S., 2020, New constraints on the last deglaciation of the Cordilleran Ice Sheet in coastal Southeast Alaska: Quaternary Research, v. 96, p. 140–160, https://doi.org/10.1017/qua.2020.32.

Letham, B., Martindale, A., Macdonald, R., Guiry, E., Jones, J., and Ames, K.M., 2016, Postglacial relative sea-level history of the Prince Rupert area, British Columbia, Canada: Quaternary Science Reviews, v. 153, p. 156–191, https://doi.org/10.1016/j.quascirev.2016.10.004.

Loney, R.A., 1964, Stratigraphy and petrography of the Pybus-Gambier area, Admiralty Island, Alaska: U.S. Geological Survey Bulletin 1178, 103 p., 1 sheet, scale 1:63,360, https://doi.org/10.3133/b1178.

Luternauer, J.L., Clague, J.J., Conway, K.W., Barrie, J.V., Blaise, B., and Mathewes, R.W., 1989, Late Pleistocene terrestrial deposits on the continental shelf of western Canada: Evidence for rapid sea-level change at the end of the last glaciation: Geology, v. 17, p. 357–360, https://doi.org/10.1130/0091-7613(1989)017<0357:LPTDOT>2.3.CO;2.

Mackie, Q., Davis, L., Fedje, D., McLaren, D., and Gusick, A., 2014, Locating Pleistocene-age submerged archaeological sites on the Northwest Coast: Current status of research and future directions, *in* Graf, K.E., Ketron, C.V., and Waters, M.R., eds., Paleoamerican Odyssey: College Station, Texas, USA, Texas A&M University Press, p. 133–147.

Mackie, Q., Fedje, D., and McLaren, D., 2018, Archaeology and sea level change on the British Columbia coast: Canadian Journal of Archaeology, v. 42, p. 74–91.

Mann, D.H., and Hamilton, T.D., 1995, Late Pleistocene and Holocene paleoenvironments of the North Pacific coast: Quaternary Science Reviews, v. 14, p. 449–471, https://doi.org/10.1016/0277-3791(95)00016-I.

Mann, D.H., and Streveler, G.P., 2008, Post-glacial relative sea level, isostasy, and glacial history in Icy Strait, Southeast Alaska, USA: Quaternary Research, v. 69, p. 201–216, https://doi.org/10.1016/j.yqres.2007.12.005.

Mathewes, R.W., Lacourse, T., Helmer, E.F., Howarth, C.R., and Fedje, D.W., 2019, Late Pleistocene vegetation and sedimentary charcoal at Kilgii Gwaay archaeological site in coastal British Columbia, Canada, with possible proxy evidence for human presence by 13,000 cal BP: Vegetation History and Archaeobotany, v. 29, p. 297–307, https://doi.org/10.1007/s00334-019-00743-4.

McConnell, R.G., 1913, Portions of Portland Canal and Skeena mining divisions, Skeena district, B.C.: Geological Survey of Canada Memoir 32, 101 p.

McLaren, D., 2008, Sea level change and archaeological site locations on the Dundas Island Archipelago of north coastal British Columbia [Ph.D. thesis]: Victoria, British Columbia, University of Victoria., 311 p.

McLaren, D., Fedje, D., Hay, M.B., Mackie, Q., Walker, I.J., Shugar, D.H., Eamer, J.B.R., Lian, O.B., and Neudorf, C., 2014, A post-glacial sea level hinge on the central Pacific coast of Canada: Quaternary Science Reviews, v. 97, p. 148–169, https://doi.org/10.1016/j.quascirev.2014.05.023.

McLaren, D., Fedje, D., Dyck, A., Mackie, Q., Gauvreau, A., and Cohen, J., 2018, Terminal Pleistocene epoch human footprints from the Pacific coast of Canada: PLoS One, v. 13, e0193522, https://doi.org/10.1371/journal.pone.0193522.

McLaren, D., Fedje, D., Mackie, Q., Davis, L.G., Erlandson, J., Gauvreau, A., and Vogelaar, C., 2020, Late Pleistocene archaeological discovery models on the Pacific coast of North America: PaleoAmerica, v. 6, p. 43–63, https://doi.org/10.1080/20555563.2019.1670512.

Miller, R.D., 1972, Surficial geology of the Juneau urban area and vicinity, Alaska, with emphasis on earthquake and other geologic hazards: U.S. Geological Survey Open-File Report 72-255, 108 p., 7 sheets, scale 1:24,000, https://doi.org/10.3133/ofr72255.

Miller, R.D., 1973a, Two diamictons in a landslide scarp on Admiralty Island, Alaska, and the tectonic insignificance of an intervening peat bed: Journal of Research of the U.S. Geological Survey, v. 1, p. 309–314.

Miller, R.D., 1973b, Gastineau Channel Formation, a composite glaciomarine deposit near Juneau, Alaska: U.S. Geological Survey Bulletin 1394-C, p. C1–C20, https://doi.org/10.3133/b1394C.

Miller, R.D., 1975, Surficial geologic map of the Juneau urban area and vicinity, Alaska: U.S. Geological Survey Miscellaneous Investigations Series Map 885, 1 sheet, scale 1:48,000, https://doi.org/10.3133/i885.

Mobley, C.M., 1988, Holocene sea levels in Southeast Alaska: Preliminary results: Arctic, v. 41, p. 261–266, https://doi.org/10.14430/arctic1730.

Peltier, W.R., and Fairbanks, R.G., 2006, Global glacial ice volume and Last Glacial Maximum duration from an extended Barbados sea level record: Quaternary Science Reviews, v. 25, p. 3322–3337, https://doi.org/10.1016/j.quascirev.2006.04.010.

Praetorius, S.K., Mix, A.C., Walczak, M.H., Wolhowe, M.D., Addison, J.A., and Prahl, F.G., 2015, North Pacific deglacial hypoxic events linked to abrupt ocean warming: Nature, v. 527, p. 362–366, https://doi.org/10.1038/nature15753.

Praetorius, S., Mix, A., Jensen, B., Froese, D., Milne, G., Wolhowe, M., Addison, J., and Prahl, F., 2016, Interaction between climate, volcanism, and isostatic rebound in Southeast Alaska during the last deglaciation: Earth and Planetary

Science Letters, v. 452, p. 79–89, https://doi.org/10.1016/j.epsl.2016.07.033.
Praetorius, S.K., Condron, A., Mix, A.C., Walczak, M.H., McKay, J.L., and Du, J., 2020, The role of Northeast Pacific meltwater events in deglacial climate change: Science Advances, v. 6, eaay2915, https://doi.org/10.1126/sciadv.aay2915.
Putnam, D.E., and Fifield, T.E., 1995, Estuarine archaeology and Holocene sea level change on Prince of Wales Island, Alaska, *in* Proceedings, Alaska Anthropological Association 22nd Annual Meeting, Anchorage, 23–25 March, Abstracts, p. 19.
Reimer, P.J., Austin, W.E.N., Bard, E., Bayliss, A., Blackwell, P.G., Bronk Ramsey, C., Butzin, M., Cheng, H., Edwards, R.L., Friedrich, M., Grootes, P.M., Guilderson, T.P., Hajdas, I., Heaton, T.J., Hogg, A.G., Hughen, K.A., Kromer, B., Manning, S.W., Muscheler, R., Palmer, J.G., Pearson, C., van der Plicht, J., Reimer, R.W., Richards, D.A., Scott, E.M., Southon, J.R., Turney, C.S.M., Wacker, L., Adolphi, F., Büntgen, U., Capano, M., Fahrni, S.M., Fogtmann-Schulz, A., Friedrich, R., Köhler, P., Kudsk, S., Miyake, F., Olsen, J., Reinig, F., Sakamoto, M., Sookdeo, A., and Talamo, S., 2020, The IntCal20 Northern Hemisphere radiocarbon age calibration curve (0–55 cal kBP): Radiocarbon, v. 62, p. 725–757, https://doi.org/10.1017/RDC.2020.41.
Riehle, J.R., Champion, D.E., Brew, D.A., and Lanphere, M.A., 1992a, Pyroclastic deposits of the Mount Edgecumbe volcanic field, southeast Alaska: Eruptions of a stratified magma chamber: Journal of Volcanology and Geothermal Research, v. 53, p. 117–143, https://doi.org/10.1016/0377-0273(92)90078-R.
Riehle, J.R., Mann, D.H., Peteet, D.M., Engstrom, D.R., Brew, D.A., and Meyer, C.E., 1992b, The Mount Edgecumbe tephra deposits, a marker horizon in southeastern Alaska near the Pleistocene-Holocene boundary: Quaternary Research, v. 37, p. 183–202, https://doi.org/10.1016/0033-5894(92)90081-S.
RGI Consortium, 2017, Randolph Glacier Inventory (RGI)—A dataset of global glacier outlines (version 6.0): Boulder, Colorado, Global Land Ice Measurements from Space, Technical Report, https://doi.org/10.7265/N5-RGI-60 (accessed August 2021).
Sainsbury, C.L., 1961, Geology of part of the Craig C-2 quadrangle and adjoining areas, Prince of Wales Island, southeastern Alaska: The general and economic geology of an area 35 miles northwest of Ketchikan: U.S. Geological Survey Bulletin 1058-H, p. 299–362, https://doi.org/10.3133/b1058H.
Schmuck, N.S., 2021, Contextualizing the development of coastal adaptations in postglacial southeast Alaska [Ph.D. thesis]: Fairbanks, University of Alaska Fairbanks, 233 p.
Schmuck, N., Reuther, J., Baichtal, J.F., and Carlson, R.J., 2021, Quantifying marine reservoir effect variability along the Northwest Coast of North America: Quaternary Research, FirstView, 15 March 2021, p. 1-22, https://doi.org/10.1017/qua.2020.131.
Shugar, D.H., Walker, I.J., Lian, O.B., Eamer, J.B., Neudorf, C., McLaren, D., and Fedje, D., 2014, Post-glacial sea level change along the Pacific coast of North America: Quaternary Science Reviews, v. 97, p. 170–192, https://doi.org/10.1016/j.quascirev.2014.05.022.
Stuckenrath, R., Jr., 1971, Report of archaeological and paleoclimatological survey, vicinity of Ketchikan, Alaska: Report on file, Radiocarbon Laboratory, Smithsonian Institution, Washington, D.C., 9 p.
Swanston, D.N., 1969, A late-Pleistocene glacial sequence from Prince of Wales Island, Alaska: Arctic, v. 22, p. 25–33.
Trüssel, B.L., Motyka, R.J., Truffer, M., and Larsen, C.F., 2013, Rapid thinning of lake-calving Yakutat Glacier and the collapse of the Yakutat Icefield, southeast Alaska, USA: Journal of Glaciology, v. 59, p. 149–161, https://doi.org/10.3189/2013JoG12J081.
Twenhofel, W.S., 1952, Recent shore-line changes along the Pacific coast of Alaska: American Journal of Science, v. 250, p. 523–548, https://doi.org/10.2475/ajs.250.7.523.
Viens, R.J., 2001, Late Holocene climate change and calving glacier fluctuations along the southwestern margin of the Stikine Icefield, Alaska [Ph.D. thesis]: Seattle, University of Washington, 160 p.
Wilcox, P.S., Addison, J., Fowell, S.J., Baichtal, J.F., Severin, K., and Mann, D.H., 2019a, A new set of basaltic tephras from Southeast Alaska represent key stratigraphic markers for the late Pleistocene: Quaternary Research, v. 92, p. 246–256, https://doi.org/10.1017/qua.2018.154.
Wilcox, P.S., Dorale, J.A., Baichtal, J.F., Spötl, C., Fowell, S.J., Edwards, R.L. and Kovarik, J.L., 2019b, Millennial-scale glacial climate variability in Southeastern Alaska follows Dansgaard-Oeschger cyclicity: Scientific Reports, v.9, no. 1, p. 1–8, https://doi.org/10.1038/s41598-019-44231-1.
Wilson, F.H., Hults, C.P., Mull, C.G., and Karl, S.M., compilers, 2015, Geologic map of Alaska: U.S. Geological Survey Scientific Investigations Map 3340, 2 sheets, scale 1:1,584,000, 196 p. text, https://doi.org/10.3133/sim3340.
Wing, B.L., Murphy, J.M., and Rutecki, T.L., 2000, Occurrence of Pacific sardine, *Sardinops sagax*, off southeastern Alaska: Fishery Bulletin, v. 98, p. 881–883.
Worl, R., 2010, Tlingit, *in* Biddison, D.D., Ongtooguk, P.C., Worl, R., and Crowell, A.L., eds., Living Our Cultures, Sharing Our Heritage: The First Peoples of Alaska: Washington, D.C., Smithsonian Books, 312 p.
Yehle, L.A., 1974, Reconnaissance engineering geology of Sitka and vicinity, Alaska, with emphasis on evaluation of earthquake and other geologic hazards: U.S. Geological Survey Open-File Report 74-53, 104 p., 3 sheets, https://doi.org/10.3133/ofr7453.
Yehle, L.A., 1978, Reconnaissance engineering geology of the Petersburg area, southeastern Alaska, with emphasis on geologic hazards: U.S. Geological Survey Open-File Report 78-675, 92 p., 2 sheets, https://doi.org/10.3133/ofr78675.
Yehle, L.A., 1979, Reconnaissance engineering geology of the Yakutat area, Alaska, with emphasis on evaluation of earthquake and other geologic hazards: U.S. Geological Survey Professional Paper 1074, 44 p., 1 sheet, scale 1:63,360, https://doi.org/10.3133/pp1074.
Yehle, L.A., and Lemke, R.W., 1972, Reconnaissance engineering geology of the Skagway area, Alaska, with emphasis on evaluation of earthquake and other geologic hazards: U.S. Geological Survey Open-File Report 72–454, 108 p., 4 sheets, https://doi.org/10.3133/ofr72454.